Master thesis

Life Cycle and Economic assessment of CO_2 mineralization pathways in Austria

Carried out for the purpose of obtaining the degree
of Diplom-Ingenieur (Dipl.-Ing. or DI)

submitted at TU Wien
Faculty of Mechanical and Industrial Engineering

by

Mahmoud Amini Khoei
Mat.No.: 12044923

under the supervision of
Univ. Prof. Stavros Papadokonstantakis
Univ.Ass.in Pingping Wang
Institute of Chemical, Environmental
and Bioscience Engineering

Place, Date _____

I confirm that the printing of this thesis requires the approval of the examination board.

Affidavit

I declare in lieu of oath, that I wrote this thesis and carried out the associated research myself, using only the literature cited in this volume. If text passages from sources are used literally, they are marked as such.

I confirm that this work is original and has not been submitted for examination elsewhere, nor is it currently under consideration for a thesis elsewhere.

I acknowledge that the submitted work will be checked electronically-technically using suitable and state-of-the-art means (plagiarism detection software). On the one hand, this ensures that the submitted work was prepared according to the high-quality standards within the applicable rules to ensure good scientific practice "Code of Conduct" at the TU Wien. On the other hand, a comparison with other student theses avoids violations of my personal copyright.

Place and Date

Signature

Acknowledgements

I would like to express my deepest gratitude to Prof. Stavros Papadokonstantakis, Head of the research unit of Process Systems Engineering for Bioresources and Sustainability, for his invaluable leadership and support. My sincere thanks also go to the entire research group for their friendship and encouragement during challenging times.

I am especially grateful to my thesis advisor, Pingping Wang MSc, for her dedicated guidance, patience, and unwavering support throughout the course of my research.

I would also like to thank Safdar Abbas MSc, for his assistance with the Activity Browser software and for his excellent collaboration in data analysis. Special thanks to Ada Josefina Robinson MSc, for her kind support.

Finally, I extend my appreciation to all members of the Institute of Chemical, Environmental and Bioscience Engineering for their ongoing support and for providing the necessary resources during my studies.

Table of Contents

English Abstract

In Austria, annual CO_2 emissions are approximately 73 million tons [1], significantly contributing to greenhouse gas concentrations. This study evaluates the environmental and economic feasibility of two carbon mineralization processes in Austria: (1) the utilization of biogenic CO_2 from biogas upgrading with recycled concrete aggregates (RCA), and (2) the carbonation of steel slag using process-generated CO_2 from steel production. A combined life cycle assessment (LCA) and techno-economic analysis (TEA) framework was applied to assess these processes, focusing on key operational parameters such as RCA particle size, CO_2 delivery pressure, and electricity sources.

For biogenic CO_2 mineralization, results indicate that coarser RCA fractions (2–4 mm) yield the lowest global warming potential (GWP) of 0.12 kg CO_2-eq per kg CO_2 mineralized, driven by reduced crushing energy. However, economic viability is highly sensitive to RCA costs and product value, with levelized costs ranging from 127.7 EUR/ton CO_2 at optimal conditions (60 bar pressure, zero RCA cost and for 0.1 kg/s CO_2). Steel slag carbonation demonstrated a GWP of 0.023 kg CO_2-eq per kg CO_2 mineralized, with levelized costs of 126.59 EUR/ton for base case (100 kg CO_2/h) and 16.10 EUR/ton for large-scale plant (e.g., Voestalpine Linz), highlighting the critical role of economies of scale.

Sensitivity analyses highlighted the dominance of energy costs and economies of scale. While both processes offer significant CO_2 sequestration potential, their deployment hinges on policy support for carbon pricing (>65 EUR/ton), subsidized energy, and valorisation of by-products (e.g., calcium carbonate). The study underscores the trade-offs between environmental benefits and financial feasibility, providing actionable insights for scaling carbon mineralization technologies in industrial applications.

Deutsche Kurzfassung

In Österreich belaufen sich die jährlichen CO_2-Emissionen auf etwa 73 Millionen Tonnen und tragen somit erheblich zur Konzentration von Treibhausgasen bei [1]. Diese Studie bewertet die ökologische und wirtschaftliche Machbarkeit von zwei Prozessen der Kohlenstoffmineralisierung in Österreich: (1) die Nutzung von biogenem CO_2 aus der Biogasaufbereitung mit rezyklierten Betonzuschlagstoffen (RCA) und (2) die Karbonatisierung von Stahlwerksschlacke unter Verwendung von prozessgeneriertem CO_2 aus der Stahlproduktion. Ein kombiniertes Rahmenwerk aus Lebenszyklusanalyse (LCA) und techno-ökonomischer Analyse (TEA) wurde angewendet, um diese Prozesse zu bewerten, wobei der Fokus auf wesentlichen Betriebsparametern wie RCA-Partikelgröße, CO_2-Druck und Stromquellen lag.

Für die Mineralisierung von biogenem CO_2 zeigen die Ergebnisse, dass gröbere RCA-Fraktionen (2–4 mm) das geringste Treibhauspotenzial (GWP) von 0,12 kg CO_2-Äquivalent pro kg mineralisiertem CO_2 aufweisen, was auf den reduzierten Energieaufwand beim Zerkleinern zurückzuführen ist. Die wirtschaftliche Tragfähigkeit ist jedoch stark abhängig von den Kosten des RCA und dem Produktwert. Die nivellierten Kosten liegen bei optimalen Bedingungen (60 bar Druck, keine RCA-Kosten und 0,1 kg/s CO_2) bei 127,7 EUR pro Tonne CO_2. Die Karbonatisierung von Stahlwerksschlacke zeigte ein GWP von 0,023 kg CO_2-Äquivalent pro kg mineralisiertem CO_2, mit nivellierten Kosten von 126,59 EUR/Tonne im Basisszenario (100 kg CO_2/h) und 16,10 EUR/Tonne für eine großtechnische Anlage (z. B. Voestalpine Linz), was die entscheidende Rolle von Skaleneffekten unterstreicht.

Sensitivitätsanalysen betonten die Bedeutung von Energiekosten und Skaleneffekten. Beide Prozesse bieten ein erhebliches Potenzial zur CO_2-Abscheidung, ihre Umsetzung hängt jedoch stark von politischen Maßnahmen wie einer CO_2-Bepreisung (>65 EUR/Tonne), subventionierter Energie sowie der Wertschöpfung von Nebenprodukten (z. B. Calciumcarbonat) ab. Die Studie hebt die Abwägung zwischen ökologischen Vorteilen und wirtschaftlicher Umsetzbarkeit hervor und liefert konkrete Erkenntnisse zur Skalierung von Technologien zur Kohlenstoffmineralisierung in industriellen Anwendungen.

.

List of Figures

List of Tables

List of Abbreviations and Symbols

ABS	Ammonium Bisulfate
AD	Anaerobic Digestion
AS	Ammonium Sulfate
BAU	business-as-usual
BECCS	Bioenergy with Carbon Capture and Storage
BOFS	Basic Oxygen Furnace slag
CAPEX	Capital Expenditures
CCS	Carbon Capture and Storage
CCU	Carbon Capture and Utilization
CDR	Carbon Dioxide Removal
CH_4	Methane
CKD	Cement Kiln Dust
CO_2	Carbon Dioxide
Cp	specific heat capacity
CRW	cold-rolling wastewater
CSTR	Continuously Stirred Tank Reactor
DAC	direct air capture
EAF	Electric Arc Furnace
FU	Functional Unit
GHG	Greenhouse Gas
IPCC	Intergovernmental Panel on Climate Change
IRR	internal rate of return
KPI	Key Performance Indicators
LCA	Life Cycle Assessment
LCI	Life Cycle Inventory
LCV	Lower Calorific Value
MCT	Mineral carbonation technology
OPC	Ordinary Portland Cement
OPEX	Operational expenditures
PB	Planetary Boundary

PCC	precipitated calcium carbonate
PV	photovoltaic
USD	United States Dollar
RCA	recycled concrete aggregate
RPB	rotating packed bed
TEA	Techno-Economic Assessment
WACC	Weighted Average Cost of Capital
η_{is}	Isentropic efficiency

1 Introduction and Motivation

Climate change is a crucial global issue that requires comprehensive responses to mitigate its impacts and ensure a sustainable future for the planet. Efforts to address climate change span various disciplines and considerations, from economic impacts to renewable energy sources and adaptation strategies. Studies have shown that the economic impact of climate change can be more than double if the phenomenon doubles [2]. Renewable energy sources play a crucial role in climate change mitigation, with reports highlighting the costs and benefits of transitioning to cleaner energy alternatives [3] . According to the Intergovernmental Panel on Climate Change (IPCC), significant volumes of carbon dioxide (CO_2) must be removed from the atmosphere for the world to achieve its climate goals. The importance of Carbon Dioxide Removal (CDR) is highlighted by the need to limit global mean temperature increase below 1.5 C, which necessitates a phase-out of CO_2 production along with the rapid upscaling of CDR technologies [4]. While traditional Carbon Capture and Storage (CCS) captures CO_2 before it enters the atmosphere (e.g., at fossil fuel plants), bioenergy with CCS (BECCS) is considered a CDR method because it combines biogenic CO_2 uptake (during biomass growth) with point-source capture [5], resulting in net-negative emissions. Thus, Bioenergy with Carbon Capture and Storage BECCS exemplifies how certain hybrid technologies bridge the gap between emission prevention and atmospheric removal. Among the various CDR approaches, BECCS is emphasized as crucial for achieving global net-zero carbon dioxide emission goals [6]. Policymakers acknowledge the need for large-scale CDR to achieve climate mitigation targets, underscoring the importance of transdisciplinary approaches in shaping the future of CDR [7].

Carbon Capture and Utilization (CCU) technologies are essential for their role in mitigating atmospheric CO_2 emissions by capturing CO_2 emissions from various sources and converting them into valuable products. CCU involves capturing from point source or ambient air and converting it into useful materials [8]. While carbon capture and storage (CCS) focuses on sequestering CO_2 for long-term storage, carbon capture and utilization (CCU) aim to repurpose CO_2 as a resource across multiple sectors, including chemical production, synthetic fuels, building materials (e.g., concrete curing), and even enhanced agricultural yields. thereby reducing the need to extract CO_2 from natural sources [9].

This shift towards CCU has gained momentum due to its potential to address climate change challenges [10]. The concept of CCU has been gaining traction as a viable solution

to greenhouse gas emission and the increasing global energy demand. By repurposing captured CO_2 as a feedstock for valuable chemicals, CCU presents a promising avenue for reducing carbon footprints [11].

One of the key advantages of CCU lies in its potential to overcome the limitation associated with CCS in terms of design complexity and operational costs [12],[13]. Moreover, the development of CCU technologies that reuse captured CO_2 has been prioritized to accelerate the deployment of CCUS initiatives [13]. By optimizing the conversation of CO_2 into valuable chemicals through innovative technologies, CCU offers a pathway towards achieving carbon neutrality and combating global warming [14]. This shift towards CCU reflects an emerging carbon circularity paradigm, where CO_2 is no longer viewed solely as a waste product but as a valuable feedstock for industrial processes. This approach aligns with and extends the broader circular economy paradigm, which emphasizes resource efficiency, closed-loop systems, and waste valorization across all material flows. Carbon capture and utilization (CCU) technologies encompass a diverse portfolio of processes aimed at mitigating greenhouse gas emissions and promoting sustainable resource management. The selection of the most suitable CCU process depends on various factors, including the source of CO_2 emissions, the desired products, economic viability, and environmental considerations [14]. As such, CCU should be viewed as a multifaceted approach that integrates different technologies to address specific challenges and opportunities in carbon management.

The importance of considering a range of CCU processes lies in the need to tailor solutions to specific contexts. In industrial regions with high point-source emissions, captured CO_2 can be utilized for diverse applications such as chemicals, construction materials, or synthetic fuels [15]. In contrast, areas with limited industrial activity may rely on direct air capture (DAC) combined with CO_2 conversion to liquid fuels, a universally demanded product, since other CCU pathways often lack feasibility without concentrated emission sources [12]. Life cycle assessments (LCA) of these processes are critical to evaluate their sustainability and guide stakeholders toward technologies offering the greatest environmental benefits [16].

In summary, the diverse portfolio of CCU processes underscores the need for a comprehensive and integrated approach to carbon management.

2 Literature Review

2.1 Introduction to CCUS/CDR

The climate crisis demands a variety of technological solutions. Carbon Capture, Utilization, and Storage (CCUS) has emerged as a crucial framework to mitigate the impacts of CO_2 emissions. Within CCUS, Carbon Capture and Utilization (CCU) is particularly notable for its potential to reduce emissions while simultaneously generating economic value. Similarly, Rosa et al. [13] emphasizes CCU's contribution to reducing dependence on fossil feedstocks.

Most CCU applications remain carbon-neutral because the CO_2 sequestered in products is often re-released during product use, limiting its long-term impact on climate change mitigation.

Table 2.1: CCU vs. CDR: Key Differences

Concept	CCU	CDR (e.g., BECCS)
CO_2 source	Fossil/Biogenic point source	Biogenic/Direct Air Capture (DAC)
Primary goal	Circular carbon use	Permanent CO_2 removal
CO_2 fate	Re-emitted (temporary)	Permanent stored (e.g., geological or mineral form)
Climate impact	Carbon neutral (if biogenic)	Net negative
Scalability	Limited by product demand	Limited by storage infrastructure
Example	Synthetic fuels, construction materials	BECCS, mineral carbonation

Despite its potential, CCU alone is insufficient for large-scale climate mitigation. Mac Dowell et al. [17] estimate that chemical CO_2 utilization could only contribute up to 1% of the total CO_2 mitigation challenge, while Enhanced Oil Recovery (EOR)-CCS may account for 4-8%. This underscores the necessity of large-scale geological sequestration to achieve meaningful emission reductions.

In contrast, Carbon Dioxide Removal (CDR) offers a fundamentally distinct approach by ensuring permanent CO_2 sequestration. While CCU establishes circular carbon pathways, CDR technologies, such as BECCS, enable net-negative emissions through geological storage, as quantified in Rosa et al. [6]. The IPCC (2018) establishes a critical threshold of >100-year storage permanence for geological sequestration, a standard unattainable by conventional CCU approaches. Mac Dowell et al. [17] further argue that achieving net-

negative emissions requires dedicated removal strategies, as CCU pathways ultimately return CO_2 to the atmosphere. While CCS provides a viable means to reduce industrial emissions, its widespread adoption faces economic and policy challenges. Mac Dowell et al. [17] emphasize that large-scale deployment requires strong financial incentives and regulatory frameworks to support long-term viability.

2.2 CCUS/CDR Technologies landscape

Various CCUS/CDR technologies have been developed to mitigate (remove) CO_2 emissions, each with different levels of maturity and applicability. The following examples illustrate key advancements in post-combustion capture, direct air capture, and bioenergy with carbon capture and storage (BECCS), highlighting their role in industrial and energy sectors.

2.2.1 Carbon Capture in Power Plants: Life Cycle Trade-offs

Yan Wang et al. [18] provide a comprehensive examination of CCS technologies integrated with conventional power generation systems through detailed LCA. Their work analyzes three primary combustion-based electricity generation methods: pulverized coal plants, natural gas combined cycle systems and integrated gasification combined cycle plants. comparing the environmental performance of post-combustion, pre-combustion, and oxy-fuel carbon capture approaches. The research reveals that while CCS technologies can reduce direct CO_2 emissions from power plants by approximately 90%, this climate benefit comes with notable trade-offs. The energy cost penalty, representing the additional energy required for capture processes, ranges substantially from 15% to 44% depending on the specific technology configuration. This cost penalty manifests most significantly in sub-critical coal plants and affects the overall system efficiency. Furthermore, the study highlights how different capture methods create distinct environmental impact profiles. Post-combustion capture using amine-based solvents like MEA, while effective for CO_2 reduction, leads to increased acidification and eutrophication potential due to solvent degradation products. Oxy-fuel combustion demonstrates superior climate performance with the lowest global warming potential among the options studied but requires careful consideration of its higher particulate matter formation potential and energy demands.

The importance of employing both LCA and techno-economic analysis (TEA) emerges clearly from this work. LCA provides the essential framework for understanding the full environmental implications of CCS deployment, moving beyond simple carbon accounting

to reveal potential trade-offs in other impact categories. Meanwhile, TEA offers crucial insights into the economic viability and practical constraints of implementing these technologies on scale. Together, these methodologies enable a more complete evaluation of CCS systems, ensuring that emission reduction strategies don't inadvertently create new environmental burdens or become economically unfeasible. Wang et al. [18] conclude that while CCS represents a vital tool for decarbonizing existing power infrastructure, its implementation requires careful technology selection and system design to balance climate benefits against other environmental impacts and energy cost penalties. Their work particularly emphasizes the value of oxy-fuel and pre-combustion approaches for new installations where lowest-emission configurations are prioritized, while acknowledging the retrofit advantages of post-combustion systems for existing plants. This comprehensive analysis underscores the necessity of interdisciplinary assessment approaches in guiding both technology development and policy decisions for carbon management in the power sector. While CCS in power plants addresses stationary emissions, decarbonizing mobile sectors like aviation requires alternative strategies. Here, CO_2-derived synfuels, enabled by either CCU or CDR, emerge as a viable pathway, albeit with distinct challenges.

2.2.2 Aviation Decarbonization: CCU vs. CDR Pathways

Becattini et al. [19] presents a comprehensive techno-economic analysis of pathways to achieve net-zero emissions in aviation through CCS and CCU technologies. Their study compares conventional fossil jet fuel (subject to carbon taxes) against four carbon-neutral alternatives: two CCS routes (direct air capture with storage/DAC-CCS and point-source biogenic CO_2 capture/PSC-CCS) and two CCU routes producing synthetic fuels from either atmospheric or biogenic CO_2. The analysis reveals PSC-CCS as the most immediately viable solution, with jet fuel costs (~0.53 EUR/L) competitive with business-as-usual (BAU) today due to efficient capture of concentrated biogenic CO_2 from waste-to-energy plants. In contrast, CCU-based routes face significant barriers, requiring 20 times more energy than CCS and producing fuel at 2.29–4.89 EUR/L. This energy intensity makes their emissions highly sensitive to grid carbon intensity, even with low-carbon electricity (e.g., France's 0.09 tCO_2/MWh), CCU emissions surpass BAU. The study's Monte Carlo analyses confirm PSC-CCS's robustness across parameter variations (±50%), while BAU costs diverge widely due to carbon price uncertainty.

Policy emerges as a critical lever: CCS becomes viable at carbon prices of 70–100 EUR/ton

CO_2, while CCU needs both high carbon prices and unrealistically cheap renewable electricity (<0.04 EUR/kWh). The study highlights synergies with waste management, showing biogenic CO_2 from waste-to-energy plants could offset ~40% of aviation emissions in some regions. While DAC-CCS may become competitive by 2035 with technological learning, PSC-CCS stands out as the most pragmatic near-term solution for decarbonizing flight.

The aviation study underscores the superiority of CDR for hard-to-abate sectors. However, in industries where CO_2 is a feedstock (e.g., chemicals), CCU may offer circularity benefits, albeit with energy trade-offs. Carbon Management in the Chemical Industry.

2.2.3 Carbon Management in the Chemical Industry

Gabrielli et al. [20] evaluates three pathways, Carbon Capture and Storage (CCS), Carbon Capture and Utilization (CCU), and BIO route, to achieve a net-zero-CO_2 chemical industry, using methanol production. The CCS route combines fossil fuels with permanent CO_2 storage, offering near-term feasibility with moderate energy demands (0.94–1.78 MWh electricity and 2.11–3.62 MWh heat per ton methanol) but requires accessible geological storage and public acceptance. This includes both point-source capture (from industrial emissions) and direct air capture variants.

The CCU pathway converts captured CO_2 into chemicals using renewable hydrogen, eliminating fossil dependence but facing steep energy requirements (10.4–10.9 MWh electricity per ton methanol). Like CCS, it can utilize either point-source CO_2 or direct air capture, with DAC-based systems requiring 15% more energy due to atmospheric CO_2 extraction costs. The BIO route, reliant on biomass carbon uptake, is inherently carbon-neutral but demands extensive land (2,500 m^2 per ton methanol annually), raising concerns about competition with food systems and ecosystems.

A critical insight is the trade-off between scalability and resource constraints: CCS leverages existing infrastructure but perpetuates fossil fuel use; CCU avoids fossils but hinges on cheap, abundant renewables; BIO is sustainable but land intensive. Under a net-zero framework, CCS and BIO show slower growth in CO_2 emissions as grid carbon intensity rises, while CCU emissions escalate 8–10 times faster due to its electricity intensity.

The study concludes that regional context, geological storage capacity, renewable energy potential, and land availability, will determine the optimal mix of these technologies, with hybrid approaches likely being most effective. Gabrielli et al. [20] identify the energy-intensity of CCU (10.4 MWh/ton methanol) as a key barrier to scalability, a limitation

mitigated in Zhang et al. (2020) [21] by coupling biogas-derived CO_2 with renewable hydrogen. Their Power-to-Methane system achieves 41–70% lower emissions than gasoline vehicles, demonstrating how sector-specific carbon cycling can bypass the fossil dependency inherent in conventional CCU.

2.2.4 Biogenic Power-to-Methane for Sustainable Fuel Production

Zhang et al. [21] conducted a life cycle assessment (LCA) of Power-to-Gas (P2G) systems utilizing CO_2 from biogas, focusing on methanation pathways and their potential for greenhouse gas (GHG) reduction in the mobility sector. The study compares three approaches: conventional biogas upgrading, methanation with CO_2 from biogas upgrading, and direct biogas methanation, evaluating their carbon footprint and feasibility as sustainable energy solutions.

The results highlight that using biomethane as a vehicle fuel could reduce GHG emissions by 27–62% compared to natural gas vehicles and 41–70% compared to gasoline-powered vehicles. However, the extent of emission reductions is highly dependent on the energy source used for electrolysis. For instance, employing hydropower-based electricity for hydrogen production could reduce emissions by up to 95% compared to conventional pathways.

A key trade-off is the limited availability of biogenic carbon sources. While biogas-derived CO_2 allows for a closed carbon cycle, enabling a more sustainable CCU (Carbon Capture and Utilization) pathway, its scalability is constrained by biomass resource availability. Furthermore, electricity demand for electrolysis significantly impacts the environmental footprint, requiring low-carbon energy sources to ensure net emissions reductions.

From an interdisciplinary perspective, the study integrates chemical engineering (methanation reactions, gas upgrading), environmental science (LCA methodologies), and energy systems analysis (grid decarbonization, seasonal energy storage needs). Additionally, economic and policy factors play a crucial role, as incentives for renewable energy deployment and carbon pricing mechanisms could determine the viability of these pathways.

The findings emphasize that while CCU via power-to-methane can contribute to decarbonization, its feasibility depends on renewable electricity availability, process efficiency, and biomass constraints. Compared to CDR (Carbon Dioxide Removal) approaches, which aim for long-term sequestration, CCU strategies such as methanation offer an alternative by integrating captured CO_2 into the energy system, reducing emissions in a circular economy model.

The circular carbon economy modeled by Zhang et al. [21], where biogas waste streams become feedstocks, aligns with Sitinjak et al. [22] finding that public support for CCUS rises when projects demonstrate local economic benefits.

Sitinjak et al. [22] shows that public awareness of CCUS remains critically low, with over 50% of surveyed respondents rating their knowledge as "poor" or "very poor," correlating with high levels of fear and skepticism. This underscores the necessity of targeted education and transparent communication to bridge the knowledge gap and build trust.

Notably, the study reveals a preference for carbon capture and utilization (CCU) over storage (CCS), as CCU is perceived as innovative, economically beneficial (e.g., job creation, product development), and environmentally safer. However, Sitinjak et al. [22] also identify persistent barriers, including distrust in energy companies and fears of CO_2 leakage or long-term risks. emphasizing that community engagement and participatory decision-making are vital to address concerns. As CCUS technologies grow pivotal for climate mitigation, the study reinforces that social acceptance hinges on proactive outreach, alignment with local values, and demonstrable safeguards. Policymakers and industry must prioritize these strategies alongside technical advancements to ensure successful deployment (Sitinjak et al. [22]. As demonstrated in the above examples, effective CCUS/CDR deployment requires navigating interconnected technical, economic, and socio-environmental factors.

The LCA studies reveal: power plant retrofits [18] face energy cost penalty trade-offs (15-44% output loss) while creating secondary impacts (2.3× acidification potential from amine solvents); aviation fuels [19] demand carbon prices >70 EUR/ton CO_2 for CCS viability while showing LCA-confirmed sensitivity to grid carbon intensity (>0.07 ton CO_2/MWh negates benefits); chemical production [20] balances land-use constraints (2500m²/ton methanol in LCA system boundaries) against renewable energy demands (10.9MWh/ton); and biogas systems [21] pivot on biomass availability and electrolysis carbon intensity (<152gCO_2eq/kWh). Recent social acceptance studies [22] further demonstrate that CCU pathways achieve 20-35% higher public approval than CCS due to visible product outputs and avoided storage risks, though this advantage is contingent on maintaining low energy penalties (<25% system efficiency loss) and clear local economic benefits. Similarly, this work examines CO_2 mineralization through the same multidimensional lens, particularly analyzing: Technical, Economic and Environmental aspects.

Beyond technical and social barriers, the deployment potential of both CCUS and CDR technologies hinges on their maturity. The Technology Readiness Level (TRL) framework

provides a standardized metric to assess this progression.

2.3 Technology Readiness Levels (TRLs): A Conceptual Framework

Technology Readiness Levels (TRLs) are a standardized metric to assess a technology's maturity, spanning from theoretical concepts (TRL 1) to full-scale commercialization (TRL 9) [23]. TRLs are commonly categorized into three innovation phases:

- Applied Research (TRL 1–3): Idea formulation to lab-scale validation
- Development (TRL 4–6): Process refinement and pilot-scale testing
- Deployment (TRL 7–9): Demonstration to industrial operation

While generic TRL scales (e.g., NASA's) offer broad guidelines, sector, specific adaptations, such as the chemical industry framework by Buchner et al. [23], incorporate technical milestones (e.g., reaction yield targets, scalability thresholds).

2.4 Introduction to CO_2 Mineralization

Mineral carbonation is a process that includes a series of chemical reactions designed to transform carbon dioxide (CO_2) into stable carbonate minerals. This method generally utilizes silicate or oxide minerals, The overarching reaction can be expressed as follows [24],[25].

$$CO_2 + \text{M-Silicate} \rightarrow \text{M-Carbonate} + SiO_2 \quad (2.1)$$

Oxide minerals also participate in reactions with carbon dioxide (CO_2) to produce carbonate minerals. These reactions involve oxide minerals containing metals such as magnesium (Mg) or calcium (Ca), which readily react with CO_2 to yield stable carbonate compounds:

$$MgO + CO_2 \rightarrow \text{Magnesite } (MgCO_3) \quad (2.2)$$

$$CaO + CO_2 \rightarrow \text{Calcite } (CaCO_3) \quad (2.3)$$

This process offers a potential permanent solution for CO_2 storage by transforming it into solid materials that remain stable over geological timescales. Mineral carbonation provides several advantages, including geochemically secure CO_2 storage with minimal leakage risks and the potential for commercializing the resulting carbonate materials. Research has demonstrated that mineral carbonation can produce stable and economically viable carbonate products, often through simpler processes compared to other carbon sequestration techniques [25]. A key aspect of CO_2 mineralization is whether it functions as a Carbon

Dioxide Removal (CDR) or Carbon Capture and Utilization (CCU) process. This classification depends on the source of CO_2 and the final fate of the mineralized products. If the carbonate minerals are stored permanently, the process contributes to CDR. However, if the carbonates are used in commercial applications (e.g., construction materials), then they fall under CCU. One of the key advantages of CO_2 mineralization for permanent storage is its high level of social acceptance. Unlike other CO_2 storage methods, which may raise concerns about leakage and long-term stability, carbonate minerals are thermodynamically stable and do not pose a risk of CO_2 re-release. This makes mineralization a secure and publicly acceptable option for long-term CO_2 sequestration, as it eliminates the uncertainty associated with geological storage methods.

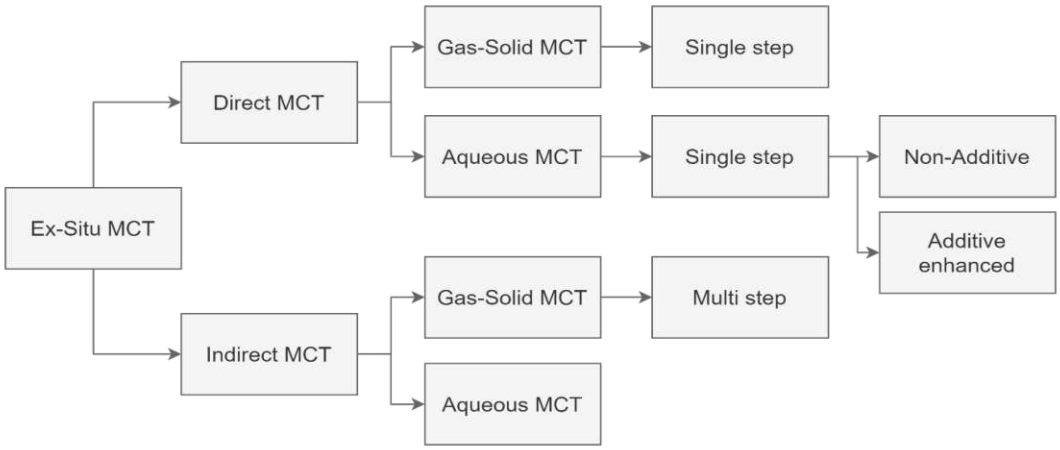

Fig. 2.1 Classification of Ex- Situ mineral carbonation Processes [26]

2.5 Direct carbonation

Direct carbonation can be classified into gas-solid carbonation and aqueous carbonation, depending on the reaction medium and process conditions. The gas-solid route process has the advantage of avoiding excessive water consumption and offering a simpler sequestration pathway. However, slow reaction rates, passivating layers forming on mineral surfaces, and Thermodynamic constraints and slow kinetics pose challenges for large-scale implementation. In contrast, aqueous direct carbonation involves dissolving CO_2 in water to form carbonic acid (H_2CO_3), which subsequently reacts with dissolved metal cations to form stable carbonate minerals. This process benefits from higher reaction kinetics due to enhanced mineral dissolution and ion mobility in solution. The fundamental reactions governing this process include:

$$CO_2+H_2O \rightarrow H_2CO_3 \quad (2.4)$$

$$Ca^{2+}+2HCO_3^- \rightarrow CaCO_3+CO_2+H_2O \quad (2.5)$$

Despite achieving higher carbonation efficiency than gas-solid methods, aqueous carbonation faces challenges related to high water consumption, energy cost intensive processing. While direct carbonation presents significant challenges, it remains a crucial area of research for CO_2 sequestration. Saran et al.[27] demonstrated that aqueous direct carbonation is a more straightforward method of CO_2 sequestration, where both the dissolution of reactive cations (e.g., Ca^{2+}, Mg^{2+}) and the carbonation reaction occur within a single reactor. In contrast to aqueous indirect carbonation, where dissolution and precipitation occur in separate steps, direct carbonation offers a simpler process design with fewer operational steps. However, this simplicity comes at the cost of slower reaction kinetics and thermodynamic limitations. Ongoing developments in process optimization, catalytic enhancements, and pressure/temperature control aim to overcome current limitations, making direct carbonation a more viable option for large-scale implementation. While direct carbonation simplifies the process by combining dissolution and precipitation, its limitations have led to the development of indirect carbonation methods, which offer greater process control and efficiency.

2.6 Indirect carbonation

Indirect CO_2 mineralization is a promising carbon sequestration method that overcomes the limitations of direct mineral carbonation by separating the process into two distinct steps:

(1) extraction of reactive ions (e.g., Ca^{2+}, Mg^{2+}) from mineral feedstocks (e.g., olivine, serpentine, industrial waste)

(2) carbonation of these ions with CO_2 to form stable carbonates (e.g., $CaCO_3$, $MgCO_3$) (Saran et al.) [27].

Unlike direct methods, which suffer from sluggish reaction kinetics due to competing dissolution and precipitation reactions in a single reactor, indirect routes enable optimized conditions for each step (e.g., acidic leaching for extraction, alkaline pH for carbonation), significantly enhancing efficiency and scalability. This approach is particularly advantageous when dealing with low-reactivity feedstocks (e.g., olivine, serpentine).

The improved reaction efficiencies gained through indirect carbonation make it a more viable option for future industrial applications. The ability to process a wider range of materials with increased effectiveness positions indirect mineral carbonation as a promising technique for large-scale implementation in carbon sequestration strategies [28]. The various mineral carbonation techniques differ in their reaction mechanisms, efficiency, and

process requirements. Table 2.1 provides a comparative overview of the key carbonation routes, highlighting their advantages, limitations, and relevant references.

Table 2.2: Mineral Carbonation: Process comparison

Route	Description	Advantages	Disadvantages	Ref.
Gas-solid (Direct)	The solid feed directly reacts with CO_2 in a process	Utilize waste materials reducing overall energy consumption	Slow reaction rates and thermodynamic	[29]
Aqueous (Direct/ Indirect)	Reaction occurs in an aqueous medium often with chemical additives	High carbonation capacity	Energy cost intensive requires expensive additives	[30]
HCl extraction (Indirect)	Hydrochloric acid (HCl) extracts reactive components from minerals	HCl is recyclable	Energy-intensive and costly	[27]
HNO_3 extraction (Indirect)	Nitric acid (HNO_3) is used to extract reactive components	Energy efficient and low cost	Non-recovery of chemicals	[31]
Molten Salt (Indirect)	Use molten salts for extraction	More energy efficient than HCl-based methods	Highly corrosive, unwanted By-products	[26]
Ammonia Extraction (Indirect)	Ammonium salts are used to extract reactive components	Produces pure products, fast reactions, and is recyclable	Expensive, limited research available	[32]

2.7 Parameters Influencing Carbonation

The kinetics of carbonation reactions are governed by a complex interplay of factors that significantly influence both the rate and mechanism of these reactions. Numerous studies have been conducted to delve into and comprehend the kinetics associated with various carbonation processes, employing a wide array of methodologies and materials. These investigations aim to elucidate how factors such as temperature, pressure, particle size, surface area, and the chemical composition of reactants impact the speed at which CO_2 is absorbed and converted into carbonate minerals. Understanding the kinetics is crucial not only for optimizing the efficiency of carbonation reactions but also for predicting the long-

term stability and effectiveness of carbon sequestration technologies.

Experimental approaches often involve monitoring reaction rates under controlled conditions, utilizing techniques such as spectroscopy, microscopy, and mass spectrometry to analyse intermediate products and reaction pathways [33]. Moreover, the choice of materials used in carbonation processes, whether natural minerals like silicates and oxides or industrial by-products, can significantly influence reaction kinetics. Each material exhibits unique properties that affect its reactivity with CO_2 and its suitability for large-scale implementation in carbon capture and storage systems [34]. By advancing the understanding of the kinetics of carbonation reactions, researchers aim to develop efficient and economically viable methods for mitigating CO_2 emissions and combating climate change. This multidisciplinary approach underscores the importance of ongoing research in optimizing carbon capture technologies and advancing sustainable practices for environmental stewardship.

2.7.1 Temperature

The carbonation reaction can be either exothermic or endothermic, depending on the specific reaction pathway and conditions. Generally, the dissolution of minerals, a critical step in carbonation, is endothermic, requiring energy input to break down the crystal structure and release reactive metal cations (e.g., Ca^{2+}, Mg^{2+}). In contrast, the precipitation of carbonate minerals (e.g., $CaCO_3$, $MgCO_3$) is typically exothermic, releasing energy as stable solid phases form [35]. Higher temperatures generally increase the reaction rate by providing the necessary activation energy for mineral dissolution. This is particularly relevant for silicate minerals, where dissolution is often the rate-limiting step [35]. Elevated temperatures enhance the release of reactive cations into solution, promoting subsequent carbonation reactions. However, as temperature increases, CO_2 solubility in pure water decreases, which can limit carbonation efficiency in aqueous systems [35]. In industrial carbonation processes, the presence of other chemical species or high-pressure conditions may alter this trend. At high temperatures, fugitive CO_2 emissions increase, and water evaporation becomes a limiting factor in aqueous systems. Additionally, the disruption of CO_2 at elevated temperatures can reduce its availability for reaction, impacting overall conversion rates. For example, studies have shown that steel slag carbonation is most effective between 50–200°C, with efficiency declining at higher temperatures [35]. Therefore, an optimal temperature range exists where the benefits of increased reaction kinetics are balanced against practical limitations such as solvent stability and process efficiency.

2.7.2 Pressure

Elevated CO_2 pressure enhances the solubility of CO_2 in water, promoting the formation of carbonic acid (H_2CO_3), a key intermediate in aqueous mineral carbonation. According to Henry's Law, the solubility of a gas in a liquid is directly proportional to its partial pressure. As pressure increases, more CO_2 dissolves in water, leading to higher concentrations of reactive carbonate species and accelerating carbonation reactions:

$$CO_2(g) \rightleftharpoons CO_2(aq) + H_2O \rightleftharpoons H_2CO_3 \rightleftharpoons HCO_3^- + H^+ \rightleftharpoons CO_3^{2-} + 2H^+ \quad (2.6)$$

Higher CO_2 pressures not only improve solubility but also shift the equilibrium of carbonation reactions toward the formation of more stable carbonate minerals [25]. In gas-solid carbonation, where reactions occur without liquid solvents, pressure critically controls both reaction efficiency and polymorph selectivity. Rugabirwa et al. [36] demonstrated that increasing CO_2 pressure (6–15 MPa) enhances vaterite formation from $Ca(OH)_2$, achieving >90% yield at 12 MPa. High pressure improves CO_2 dissolution in molten urea, facilitating reactant contact and stabilizing metastable vaterite. However, excessive pressure (>15 MPa) shows diminishing returns, as kinetic barriers (e.g., urea decomposition) begin to offset gains in carbonation efficiency. Abbas et al. [26] show that optimal carbonation occurs at a balance of pressure and temperature, as excessively high pressures without sufficient temperature activation led to slower kinetics due to passivating carbonate layers. For example, direct aqueous carbonation of serpentine or olivine achieves high conversion rates (~80–92%) at 150 atm and 185°C, but excessively high pressures (>150 atm) without sufficient thermal activation (e.g., <150°C) can lead to passivating carbonate or silica layers, reducing reaction kinetics by limiting ion diffusion to mineral surfaces. Industrial applications use high-pressure reactors (autoclaves) to facilitate mineral carbonation by maintaining CO_2 in a reactive state. However, while higher pressure and temperature improve reaction rates, maintaining these conditions requires significant energy input. Therefore, optimizing pressure and temperature together is essential to balancing reaction efficiency and operational costs [26].

2.7.3 Particle Size

Smaller particles have a higher surface area to volume ratio compared to larger particles. This increased surface area provides more reactive sites for the carbonation reaction. Experimental data from Huijgen et al. [37] demonstrates this effect clearly: reducing steel slag particle size from 2 mm to 38 µm increased CO_2 sequestration efficiency from 24% to 74%. The study further quantified this relationship, showing that halving the mean particle size

boosts reaction rates by 32–62%, depending on temperature. This dramatic improvement stems from the expanded reactive surface area in finer particles, which facilitates faster calcium leaching and carbonate formation. Finer particles dissolve more rapidly, making more cations available for reaction with CO_2 [38]. In smaller particles, the diffusion path for CO_2 and other reactants is shorter. This facilitates faster transport of reactants to the reaction sites and the removal of products from these sites, enhancing the overall reaction rate.

This is critical in aqueous carbonation, where CO_2 must dissolve in water before reacting with dissolved metal cations. Grinding minerals to a smaller size requires energy, and the energy costs can be significant. There is a trade-off between the increased reaction rate and the energy input required for particle size reduction. While smaller particles generally improve reaction rates, there is an optimal particle size range where the benefits of increased surface area and enhanced dissolution rates are balanced against energy costs and practical handling issues [37],[39].

Cost=f (Energy Input, Efficiency, Additives, Processing Factors...) (2.7)

2.7.4 Additives

Chemical additives play a crucial role in accelerating the kinetics of mineral carbonation reactions by altering the surface properties of minerals and enhancing their reactivity toward CO_2. These additives, which include acids, bases, and salts, can modify the physical and chemical characteristics of mineral surfaces, such as porosity, surface area, and charge distribution. Such modifications facilitate CO_2 adsorption and reaction by increasing the availability of active sites and improving the penetration of CO_2 into the mineral structure. Additionally, additives can dissolve or disrupt passivating layers that inhibit reaction progress, further promoting carbonation efficiency.

For instance, Zhao et al. [40] investigated the effect of various chelating agents (e.g., acetic acid, gluconic acid) on the dissolution kinetics of wollastonite ($CaSiO_3$), a calcium-bearing silicate mineral. Their study demonstrated that certain additives significantly enhance calcium extraction, a critical step in carbonation, even at low concentrations (e.g., 0.006 M). Notably, acetic acid achieved a 17.4% calcium extraction within just 6 minutes, highlighting the potential of additives to optimize reaction rates. However, the effectiveness of additives depends on their chemical properties and compatibility with the target mineral. For example, oxalic acid, despite its strong chelating ability, performed poorly due to the low

solubility of calcium oxalate, which precipitated and limited further dissolution. By accelerating reaction rates and improving process efficiency, chemical additives can reduce the energy demand and operational costs associated with large-scale mineral carbonation. This makes them a promising tool for scaling up CO_2 sequestration technologies. Future research could explore synergistic effects of combined additives or their application to industrial waste materials (e.g., steel slag) to further enhance feasibility.

2.7.5 Role of Aqueous Solutions in Carbonation

Mineral carbonation can occur in both aqueous and gas-solid environments; however, aqueous systems are often emphasized due to their facilitation of CO_2 sequestration through three essential mechanisms. First, CO_2 dissolves in water to form carbonic acid, which then dissociates into reactive species through equilibrium reactions (2.6). Simultaneously, water mediates the breakdown of mineral matrices, particularly evident in the hydrolysis of calcium-bearing phases:

$$CaO + H_2O \rightarrow Ca(OH)_2 \quad (2.8)$$

$$Ca(OH)_2 \rightarrow Ca^{2+} + 2OH^- \quad (2.9)$$

The released cations then combine carbonate species through two primary pathways:

$$Ca^{2+} + CO_3^{2-} \rightarrow CaCO_3 \quad (2.10)$$

$$Ca^{2+} + 2HCO_3^- \rightarrow CaCO_3 + CO_2 + H_2O \quad (2.11)$$

The water content significantly impacts carbonation efficiency through competing effects. The study by Pan et al. [41] using cold-rolling wastewater (CRW) in a rotating packed bed reactor (RPB) demonstrated the critical importance of water content optimization. Their results showed that:

- Insufficient water (<20 mL/g liquid-to-solid ratio) limited Ca^{2+} leaching <500 ppm
- Excess water (>20 mL/g) diluted reactant concentrations, reducing reaction rates

The optimal balance (20 mL/g) achieved: Complete mineral surface wetting without flooding, Maximum Ca^{2+} concentration (2600 ppm), Carbonation efficiency of 0.195-ton CO_2/ton slag and Energy consumption of 707 kWh/ton CO_2.This work specifically highlights how industrial wastewater can enhance carbonation through its native chemistry. CRW's natural alkalinity (pH 11.2-11.9) and ionic content (Na^+, Cl^-) improved calcium leaching while maintaining ideal conditions for carbonate formation. RPB configuration further optimized gas-liquid contact and mass transfer, demonstrating the practical potential of aqueous-phase mineral carbonation for industrial CO_2 sequestration.

These optima reflect fundamental trade-offs: steel slag's moderate-temperature aqueous processing balances energy and yield, while RCA's gas-solid routes prioritize low-energy operation at the expense of slower kinetics. Such comparisons underscore the need for feedstock-specific reactor design. These parameter optimizations (temperature, pressure, additives) directly influence the environmental and economic viability of mineral carbonation. The following Life Cycle Assessment (LCA) and techno-economic analyses (TEA) quantify these trade-offs, translating laboratory efficiencies into real-world feasibility.

2.8 Life Cycle Assessment (LCA)

Life Cycle Assessment (LCA) offers a comprehensive perspective on the environmental consequences linked to processes. This includes evaluating impacts from initial raw material extraction through to the final stages of disposal or potential recycling [42].

It plays a crucial role in pinpointing environmental hotspots within mineral carbonation processes, such as energy consumption, greenhouse gas emissions, and resource depletion. By identifying these critical areas, it facilitates targeted improvements aimed at minimizing environmental footprints effectively. LCA allows for the comparison of different carbon reduction methods and technologies, as well as alternative uses of by-products, to determine the most sustainable option. It aids decision-making by quantifying environmental benefits associated with mineral carbonation processes, such as CO_2 sequestration potential and reductions in landfill waste, while also assessing potential trade-offs involved.

The system boundaries can be adjusted depending on the study's objectives. For example, a cradle-to-cradle approach extends this scope by incorporating recycling or reuse, thereby supporting circular economic principles. Alternatively, a cradle-to-gate analysis may be employed when only impacts up to a certain production stage (e.g., factory gate) are relevant, such as in comparative assessments of intermediate products. More narrowly defined approaches include gate-to-gate, which focuses on a single process, and gate-to-grave, which evaluates impacts from a specific midpoint (e.g., waste treatment) to end-of-life disposal [43].

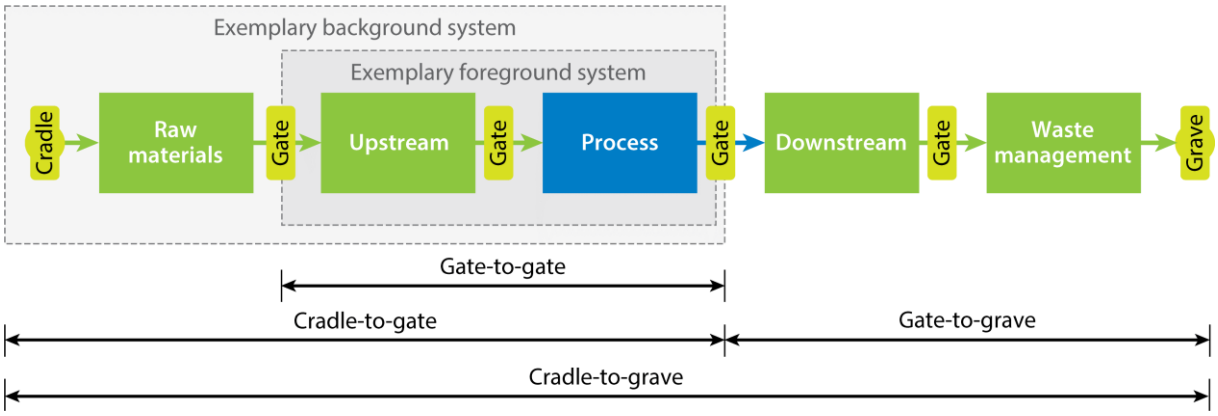

Fig. 2.2 Common System Boundary Frameworks in Life Cycle Assessment [43]

2.8.1 Functional Unit

A fundamental element of any Life Cycle Assessment is the definition of the functional unit (FU), which serves as a standardized reference to which all input and output data are normalized. It enables consistent and meaningful comparisons across different systems, products, or processes. In chemical and industrial applications, the functional unit is often defined as "1 kg of product," but its selection must reflect the core function of the system under analysis. For instance, when comparing fuels with different heating values, using "1 MJ of delivered energy" as the FU ensures comparison based on functional performance rather than mass. The choice of FU significantly influences the interpretation of LCA results and must align with the study's goal and scope. It also supports transparency and reproducibility by clearly stating the basis for impact calculations and comparisons [43].

2.9 Insights from LCA and TEA Studies

Rosa et al. [13] identified a critical CCU/CCS trade-off: mineral carbonation reduces Global Warming Potential (GWP) by 4–48%, its environmental footprint varies with process design (e.g., acidification spikes in amine-based systems). This underscores the need for integrated LCA-TEA frameworks. While Rosa et al. [13] revealed system-level trade-offs, Kirchofer et al. [44] quantified the life-cycle impacts of different alkalinity sources in aqueous mineral carbonation under the assumption of 1000 t-CO_2/day input. Their study demonstrated that various sources could achieve significant net CO_2 reductions; however, the required feedstock masses and processing energy vary substantially across materials. Cement kiln dust (CKD) showed the highest mitigation potential at 858 t-CO_2/day net storage, followed by olivine (747 t-CO_2/day), steel slag (656 t-CO_2/day), fly ash (552 t-CO_2/day), and serpentine (346 t-CO_2/day). They emphasized that maximizing the extent of

reaction is critical for improving process efficiency, with heating, mixing, and grinding identified as key energy drivers. Their findings suggest that detailed process modeling is necessary to optimize carbonation pathways and assess broader system impacts. Beyond feedstock comparisons, Fernández-González et al. [45] advanced LCA methodologies for emerging decarbonization technologies by integrating Planetary Boundaries (PBs) into life-cycle assessment (LCA). Their work highlights the importance of combining traditional environmental metrics with absolute sustainability indicators through LCA-PB. In a case study on the electrochemical reduction of CO_2 to formic acid (HCOOH), they showed that system performance is mainly influenced by energy efficiency. Switching to low-carbon electricity, such as photovoltaic (PV) solar energy, reduced the global warming potential (GWP) of CO_2-based HCOOH from 9.14 kg CO_2/kg to 1.97 kg CO_2/kg. Further electrification of heat supply lowered GWP even more, down to 0.35 kg CO_2/kg, approaching carbon neutrality. However, the fossil-based production route still performed significantly better in terms of land use, with the CO_2-based route showing a 264% higher land occupation. These results suggest that further improvements in separation technologies and electrolyze materials are necessary to achieve a truly sustainable alternative.

Even if environmental sustainability aspects constantly gain attention, assessing the economic feasibility of implementing mineral carbonation processes via techno-economic analysis (TEA) plays always a major role. While LCA identifies environmental hotspots, techno-economic analysis (TEA) translates these findings into financial viability. Hitch et al. [46] applied this to mining-integrated carbonation, showing the financial viability of integrating mineral carbonation into mining operations as a method for carbon sequestration. They developed a cost model estimating the operating cost at 82.51USD/t CO_2 and projected a net present value (NPV) of 131.5 million USD with an internal rate of return (IRR) of 25.1% under a cap-and-trade program with a carbon price of 200 USD/ton by 2027. The study highlights that maximizing sequestration efficiency and minimizing CO_2 emissions during the process are key factors for success.

Complementing Hitch's site-specific analysis, Vega et al. [47] assessed the industrial-scale potential for CO_2 conversion technologies, estimating that by 2030, e-fuel production could utilize up to 10.7 Gt of CO_2 annually, while solid carbonate production could account for around 3 Gt of CO_2 annually, particularly through the synthesis of methanol, methane, and construction materials. They emphasize the urgent need to bridge research and development gaps, reduce the cost of renewable energy, and improve CO_2 capture and green hydrogen production. Advances in catalyst materials and reactor designs are identified as

crucial for improving energy efficiency and scalability. The authors also highlight the importance of integrating life cycle assessments (LCA) and techno-economic analysis (TEA) to ensure the environmental and economic sustainability of emerging CO_2 conversion technologies.

Zhou et al. [48] shows that urea production offered the lowest unit abatement cost (29–71 USD/ton CO_2), with this range stemming from differences in capture costs across industries, chemical plants (high-purity CO_2) achieved the lower end (~29 USD/ton), while cement and power plants (low-purity CO_2) incurred higher costs (~71 USD/ton). By comparison, methanol production (59 USD/ton) and cement curing (48 USD/ton) had fixed break-even values, while microalgae cultivation (270 USD/ton) remained prohibitively expensive due to energy demands. Storage options like CO_2-ECBM (Enhanced Coalbed Methane Recovery) are profitable (-5.59 USD/ton) and saline aquifers (10 USD/ton) were viable but limited by scale. Ultimately, urea production's cost variability reflects its adaptability across sectors, and its mature technology (TRL 9), negative break-even potential (-99 USD/ton), and high emission reductions (up to 80%) solidify it as the most scalable and economically resilient solution.

The successful implementation of these solutions depends critically on technological maturity (TRL), scalability, and process efficiency factors that significantly impact overall project cost-effectiveness and success rates [47]. Through comprehensive techno-economic assessment (TEA), stakeholders can effectively anticipate and mitigate financial obstacles, enabling informed decision-making for mineral carbonation technology deployment.

2.10 Studies in CO_2 Mineralization: Bridging Theory and Industrial Deployment

Having established the fundamental mechanisms and reaction pathways of CO_2 mineralization, we now examine its practical implementation across multiple scales. The following case studies reveal how these principles are adapted from laboratory experiments to industrial deployment, with each scale presenting unique challenges and solutions. We explore bench-scale innovations in reactor design, pilot-scale demonstrations of feedstock optimization, and commercial-scale achievements in energy integration. Together, these examples provide a picture of the technology's maturation, from scientific discovery to engineering implementation, while highlighting the critical scaling factors that determine real-world viability.

Wang et al. [49] demonstrate that steel slag carbonation offers a dual solution for industrial

waste management and greenhouse gas reduction, with performance directly linked to specific processing conditions. Their research establishes that aqueous carbonation achieves optimal results when maintaining precise water content control, where a low-liquid system (0.4 L/kg) captures 180 g CO_2 per kg slag (representing 50% calcium conversion) at moderate temperatures of 50°C and 3 bar CO_2 pressure. This configuration proves significantly more effective than conventional approaches, as excessive water content reduces reaction efficiency even under more extreme conditions.

The study identifies particle size as a crucial determinant of carbonation efficiency, showing that finely ground slag particles below 38 µm can achieve exceptional CO_2 uptake of up to 75% (300 g/kg) under optimized pressure and temperature conditions. In contrast, larger particles above 200 µm demonstrate dramatically reduced sequestration capacity, highlighting the importance of material preparation in the carbonation process. The research documents how particle size reduction can improve CO_2 uptake by an order of magnitude under identical reaction conditions. Wang et al. [49] reveal that basic oxygen furnace (BOF) slag exhibits superior carbonation performance due to its favorable chemical composition. The processed material develops impressive mechanical properties, with carbonated slag bricks reaching compressive strengths of 70.6 MPa after treatment while simultaneously reducing porosity to 16.67%. This transformation effectively stabilizes reactive components that traditionally limited steel slag applications in construction materials. The technology readiness assessment within the study indicates that while laboratory-scale carbonation processes are well understood (TRL 4), pilot-scale implementations (TRL 5-6) have demonstrated technical feasibility for specific applications like brick production. Wang et al. [49] conclude that the most effective carbonation approach combines finely ground slag particles (<38 µm) with controlled water content systems (0.4 L/kg) at moderate temperatures (50-60°C) and CO_2 pressures (3-20 bar). Their analysis suggests this balanced method could potentially sequester 5-10% of steel industry emissions while producing high-value construction materials. The study emphasizes the need for further development in process standardization and secondary effect mitigation to facilitate broader industrial adoption of this promising technology.

The research highlights steel slag carbonation as a significant opportunity for circular economy implementation in heavy industry, capable of addressing both environmental concerns and material performance requirements. With global steel production generating massive quantities of slag annually, the findings present a practical pathway for simultaneous waste

valorization and carbon emissions reduction. Future work should focus on scaling challenges and environmental impact optimization to realize the full potential of this technology. Steel slag's high calcium content makes it a prime candidate for mineral carbonation, but optimal process conditions vary significantly.

While Wang et al. [49] demonstrated that aqueous carbonation achieves maximal CO_2 uptake (180 g/kg) in low-water systems (0.4 L/kg), Baciocchi et al. [50] revealed the trade-off between sequestration efficiency and leaching. They demonstrated that steel slag can effectively sequester CO_2 through direct aqueous carbonation, with performance heavily dependent on water content and reaction conditions. Their comparative study of two aqueous approaches - a water-lean "wet" method (0.4 L/kg) and a water-rich slurry (10 L/kg), revealed critical insights into industrial implementation. The low-liquid wet system achieved superior results, capturing 180 g CO_2 per kg slag (50% calcium conversion) at moderate 50°C and 3 bar CO_2 pressure. This optimized configuration benefited from concentrated conditions that promoted carbonate saturation while minimizing energy inputs. In contrast, the slurry system's higher water content (10 L/kg) proved counterproductive, yielding only 140 g CO_2/kg even under more extreme conditions (up to 150°C and 19 bar), as excess water diluted reactive species and hindered precipitation.

Mineralogical analysis showed the process selectively converted calcium phases (Ca_2SiO_4, Ca-Al oxides) to calcite, while magnesium components remained largely unreactive. An important trade-off emerged in leaching behavior: while carbonation reduced heavy metal mobility, it increased fluoride release beyond regulatory limits due to cuspidine dissolution, a critical consideration for environmental compliance. The findings establish that aqueous carbonation works best when minimizing water usage (0.4 L/kg wet system) rather than employing conventional slurry approaches. This water-efficient method could sequester approximately 5% of steel production emissions without complex chemistry or extreme conditions. However, the study highlights fluoride management as a key challenge requiring attention for practical deployment, suggesting potential need for secondary treatment steps or process modifications to address this limitation while maintaining the method's simplicity and cost advantages.

subsequent research by Pan et al. [51] extended the value chain by transforming carbonated slag into cementitious materials, highlighting the circular economy potential. The study demonstrated that electric arc furnace slag (EAF), currently a waste product, can be transformed through accelerated carbonation into two marketable resources: (1) a permanent

CO_2 sink (0.38 kg CO_2/kg slag stored as stable carbonates) and (2) supplementary cementitious materials (SCMs) that directly displace ordinary portland cement (OPC) in construction. The 138 million tons of annual CO_2 reduction potential combines both mechanisms: approximately 40% comes from direct mineralization (CO_2 permanently bound in carbonates), while 60% stems from avoiding OPC production emissions (0.73-1.00 t-CO_2/t-cement) through clinker substitution.

Their rotating packed bed reactor (RPB) achieved 83.7% carbonation conversion under moderate conditions (50-55°C, 1.03 kg/cm²), transforming unstable CaO/$Ca(OH)_2$ into calcite while reducing heavy metal leaching by 37-50%. The resulting SCMs demonstrated superior performance in blended cement (10% substitution), meeting ASTM C109 strength standards while reducing autoclave expansion below 0.8% - effectively replacing 10% of traditional cement mixes without performance trade-offs.

A critical trade-off emerged in fluoride leaching from cuspidine dissolution during carbonation, requiring potential post-treatment despite improved material stability. The water-efficient system (liquid-to-solid ratio 25 mL/g) outperformed conventional slurry approaches, with finer slag particles (<15 µm) enhancing reaction kinetics. Global implementation shows promise in steel-intensive regions like Asia-Pacific (94.9 Mt/year potential) and China (74.9 Mt/year), where both steel slag availability and cement demand are concentrated. The study establishes this waste-to-resource pathway at TRL 5-6, with the carbonated slag's dual value proposition (as both emissions mitigation tool and cement substitute) creating economic incentives for adoption. Future work must address energy optimization for grinding/heating to ensure net-negative emissions, while maintaining the quality standards required for large-scale cement displacement. Blast furnace slag (BFS) presents additional challenges. Eloneva et al. [31] introduced acetic acid leaching for BFS, but the high energy demand for NaOH regeneration (emitting 6–13 times more CO_2 than it stores) hindered scalability. They investigated the indirect aqueous carbonation of blast furnace slag (BFS) using acetic acid leaching to extract calcium, followed by CO_2 precipitation to form calcium carbonate. Experiments were conducted at 30–70°C and CO_2 pressures of 1–30 bar, with sodium hydroxide (NaOH) added to adjust pH. Results showed that calcium carbonate precipitation was negligible without NaOH, but adding 19–76 g NaOH per liter of calcium acetate solution (derived from BFS) achieved 19–74% calcium conversion. The highest yields occurred at pH ~12, regardless of temperature or pressure. The precipitates contained 60–90% calcium carbonate but were contaminated with magnesium,

silicon, and aluminum, making them unsuitable for high-purity precipitated calcium carbonate (PCC) without further purification. Thermodynamic modelling aligned with experimental results, predicting near-complete calcium conversion at high NaOH doses. Process calculations estimated that binding 1 kg of CO_2 required 4.4 kg of BFS, 3.6 L of acetic acid, and 3.5 kg of NaOH, yielding 2.5 kg of 90% pure calcium carbonate. However, the energy-intensive regeneration of NaOH and acetic acid evaporation would likely emit 6–13 times more CO_2 than the process sequesters, rendering it impractical for large-scale CO_2 storage unless waste heat or alternative alkalis are utilized. The study highlighted the trade-off between achieving high-purity carbonates and net CO_2 reduction, emphasizing the need for process optimization to address energy and chemical consumption.

While Eloneva et al.'s [31] leaching approach achieved 74% calcium conversion, its prohibitive NaOH demand undermined scalability, Yin et al. [52] circumvented this by introducing ammonium sulfate (AS) as a recyclable reagent, reducing chemical waste, though the 102 kJ/mol activation energy for AS decomposition posed a new thermal challenge. Yin et al. [52] studied the indirect carbonation of blast furnace slag (BFS) using ammonium sulfate (AS) as a recyclable reagent, focusing on the roasting stage where AS decomposes into ammonium bisulfate (ABS) to extract calcium and magnesium. The experiments were conducted at 260–380°C with an AS/BFS/SiO_2 mass ratio of 8:1:4 to prevent reactant collapse. Results showed AS decomposition was the rate-limiting step, with an activation energy of 102 kJ/mol in the presence of BFS, while the subsequent ABS-BFS reaction was rapid. Magnesium extraction reached 70% at temperatures above 340°C, while aluminium extraction peaked at 57%. The exothermic reaction between ABS and BFS partially offset the energy required for AS decomposition, improving overall efficiency. The study proposed a reaction mechanism where ABS penetrates a porous product layer ($CaSO_4$/SiO_2) to react with unreacted BFS cores. Although the process demonstrated potential for CO_2 mineralization by converting extracted Ca/Mg into stable carbonates, the work remained at lab scale without lifecycle or economic assessments.

Key parameters included temperature (optimal range: 340–380°C) and AS/BFS ratio, but the energy demands of scaling up were not quantified. Compared to direct carbonation methods, this approach avoids high-pressure CO_2 but introduces additional steps, such as roasting and leaching, which may affect feasibility. The findings highlight the trade-offs between energy efficiency and process complexity in indirect mineralization routes.

The principles developed for slag carbonation can extend to mining wastes, albeit with

lower yields. Molahid et al. [53] demonstrated that iron ore tailings, despite their low CaO content (7–15%), could sequester CO_2 under mild conditions (1 bar, 80°C), leveraging Fe-rich phases. However, the 44.9 g CO_2/kg uptake pales next to steel slag, underscoring the feedstock-reactivity trade-off.

Mineral carbonation need not rely solely on industrial byproducts. Recycled concrete aggregate (RCA), often landfilled, presents an underutilized sink. Tiefenthaler et al. [54] established RCA as an effective CO_2 sink through gas-phase mineralization, demonstrating how particle size distribution and process integration collectively govern sequestration efficiency. This study forms the foundation for one of the key objectives in this thesis: evaluating the feasibility of process designs through combined Life Cycle Assessment (LCA) and Techno-Economic Analysis (TEA) for biogenic CO_2 utilization via RCA mineralization in Austria, with explicit focus on optimizing different RCA size fractions (see Chapter 3 for detailed methodology). Their comprehensive study spanning controlled lab experiments, industrial-scale validation, and life cycle assessment revealed that finer RCA fractions (0-4mm) absorb CO_2 six times faster than coarse aggregate (4-16mm), with the 0-1mm fraction contributing disproportionately to carbonation. This size-dependent performance stems from two synergistic factors: the greater surface area of smaller particles exposes more reactive cement phases (portlandite and C-S-H), while the concrete crushing process naturally concentrates cement paste in finer fractions.

The research team validated these findings through industrial implementation, achieving TRL 7-8 by developing a complete operational chain from biogenic CO_2 sourcing to concrete production. Their system processed 120 tons RCA daily in 34m^3 reactors, mineralizing 7.2g CO_2/kg RCA at 95% efficiency while maintaining material performance standards (EN 206).

The study identified critical implementation trade-offs requiring careful balancing. First, while reducing particle size below 4mm maximizes CO_2 uptake, excessive grinding may compromise the material's structural reuse potential. Second, the current reliance on biogas-derived CO_2 (limited to ~50,000t/year in Switzerland) creates a supply bottleneck until waste incineration or direct air capture sources scale up post-2030. Life cycle assessment confirmed the technology's strong net-negative emissions profile (936kg CO_2 removed per ton stored), though regional variations in electricity carbon intensity can reduce the 93.6% carbon removal efficiency by nearly 20% in high-emission grids.

With commercialization underway through spin-off neustark AG, this work presents a rare

example of negative emission technology achieving near-commercial readiness while leveraging existing material flows. The projected 560,000t CO_2/year sequestration potential in Switzerland by 2050 - representing 30% of national negative emission requirements, highlights how particle-size optimized carbonation could transform demolition concrete from waste into a strategic climate solution, provided the balance between sequestration efficiency and material functionality is carefully maintained in real-world applications.

Zhan et al. [55] showed CO_2 curing could upgrade RCA's mechanical properties. They demonstrated an innovative CO_2 curing process that simultaneously upgrades recycled concrete aggregates (RCA) while permanently sequestering carbon dioxide. Their research explored accelerated carbonation of RCA, achieving a sequestration capacity of 12.27–44.92 g CO_2/kg aggregate, comparable to natural carbonation rates but achieved in just 2–4 hours under optimized conditions (80°C, 10 kPa CO_2 pressure). At the core of this breakthrough is a simple yet effective mechanism: exposing RCA to concentrated CO_2 transforms weak cement mortar into a densified matrix through two key reactions:

(1) $Ca(OH)_2 + CO_2 \rightarrow CaCO_3 + H_2O$ (11.8% solid volume increase) and

(2) CSH gel carbonation forms additional calcium carbonate and silica gel.

In their laboratory-scale system (33L curing chamber), the process delivered measurable improvements across all RCA grades tested. For typical RCA derived from 30 MPa concrete, the treatment reduced water absorption by 16% (from 5.25% to 4.41%), increased density by 2% (2619 to 2670 kg/m³), and decreased porosity by 1.7 percentage points, critical enhancements that address the primary limitations of recycled aggregates. The carbonation efficiency reached 56% for fine RCA (5–10 mm) due to greater surface area, though diminished to 37% for coarse aggregates (14–20 mm), revealing a size-dependent optimization opportunity.

What distinguishes this approach from conventional RCA treatments is its dual environmental benefit. Unlike methods that strip away mortar (acid washing) or coat aggregates (silica fume impregnation), CO_2 curing strengthens the existing mortar while sequestering CO_2 at a rate of up to 45 g/kg RCA. When scaled to China's annual construction waste generation (200 million tons of concrete debris), this could theoretically mineralize 9 million tons of CO_2 annually while producing higher-value aggregates. The process operates at mild temperatures (80°C) and near-ambient pressure (10 kPa), requiring less energy than steel slag carbonation (typically 50–55°C at 1.03 bar) or coal slag processing.

Key operational insights emerged from parameter optimization:

3.37% moisture content (stockpiled RCA condition) maximized carbonation, while oven-

dried or saturated aggregates showed 50% lower uptake

80% of carbonation occurred within the first 2 hours, with diminishing returns thereafter

Fine aggregates (<10 mm) achieved 1.5× faster carbonation than coarse fractions

With the construction industry generating over 1 billion tons of concrete waste annually globally, this TRL 4–5 technology presents a scalable pathway to close the materials loop. Future development should focus on (1) industrial-scale reactor design for continuous processing, (2) integration with precast concrete plants for localized recycling, and (3) lifecycle analysis to quantify net carbon benefits. By transforming both waste concrete and CO_2 into value-added materials, this process exemplifies the circular economic potential for the built environment.

Ben Ghacham et al. [56] further refined this via aqueous carbonation, though the 19 bar pressure requirement raised energy concerns. Ben Ghacham et al. [56] developed an optimized process for CO_2 sequestration using waste concrete through direct aqueous mineral carbonation. The study achieved maximum efficiency (0.078 g CO_2/g sample) under moderate conditions of 19 bar pressure and 10:1 liquid-to-solid ratio, demonstrating that higher pressures (8.25-19.30 bar) and increased slurry dilution (L/S 2.5-10 w/w) significantly improved reaction rates while maintaining ambient temperature operation, a key advantage for energy efficiency.

The researchers introduced an innovative separation approach, crushing and sieving waste concrete to isolate the reactive fine fraction (<500 µm) containing cement paste from inert aggregates. This strategy doubled in value: the cement-rich fines achieved 75% CO_2 removal (0.057 g/g) due to their high surface area and calcium content, while the recovered aggregates (>2 mm) maintained quality for construction reuse. Particle size optimization proved crucial - though grinding enhanced reactivity, even unprocessed fines reached 0.043 g CO_2/g, offering a potential energy-saving alternative.

The process showed particular promise for industrial integration by successfully using simulated flue gas (18% CO_2), eliminating the need for expensive gas purification. However, limitations emerged in the form of relatively low CO_2 uptake capacity per mass unit and unquantified energy costs for the required preprocessing steps. While thermogravimetric analysis confirmed effective conversion to stable calcium carbonates, the study identified critical knowledge gaps regarding scale-up feasibility, particularly the energy balance of water renewal and gas cycling in continuous operation.

Key operational parameters were thoroughly characterized:

- Optimal pressure range: 8.25-19.30 bar (balancing equipment costs with reaction

efficiency)

- Liquid/solid ratio: 2.5-10 w/w (higher ratios improved mass transfer)
- Reaction time: Just 10 minutes for processed fines (enabling rapid processing)

The technology presents compelling advantages for sustainable construction waste management, including dual waste valorisation and operation with impure CO_2 streams. However, its commercial viability depends on resolving the trade-off between the simplicity of direct carbonation and the current limitations in sequestration density. Further research should focus on lifecycle assessment and pilot-scale validation to address these remaining challenges.

The most radical departure from conventional approaches comes from Yu et al. [57], who paired CO_2 mineralization with resource recovery. Their NH_4Cl chemical looping process converted coal slag into calcium carbonate and extracted aluminum (62.3% yield), all at ambient pressure. This dual-output strategy may redefine economic viability for low-value feedstocks. Yu et al. [57] demonstrated a breakthrough chemical looping process that simultaneously converts coal gasification slag into valuable materials while permanently sequestering CO_2. Their research explored CO_2 mineral carbonation using coal gasification slags, achieving a sequestration potential of 121 g CO_2/kg slag, higher than steel slag (90 g/kg) and red mud (53 g/kg), though lower than carbide slag (206 g/kg). At the heart of this innovation lies a regenerable NH_4Cl system that achieves multiple objectives through elegant chemistry: when heated to 220-380°C, the ammonium chloride decomposes into HCl for metal extraction and NH_3 for CO_2 mineralization, then reforms after completing the loop.

In their 1 kg CO_2/h pilot system, this approach produced calcium carbonate particles (1-10 µm) while extracting 62.3% of the slag's aluminum content as a 47.8% Al_2O_3 concentrate, all under remarkably mild ambient pressure conditions with pH maintained between 10.6-11.0. The numbers speak to the process's efficiency: 90% CO_2 conversion, 74.8% calcium utilization, and 75-86% NH_4Cl recovery rates that make chemistry truly circular. Each metric ton of slag yields 344.5 kg of marketable calcium carbonate alongside 328.2 kg of aluminum-rich material, enabling multi-resource recovery and sustainable waste management.

What sets this apart from other mineralization approaches is its dual-product output that creates economic viability, the aluminum recovery offsets costs while the calcium carbonate provides additional revenue, all while achieving permanent carbon storage. The

system's ambient pressure operation and efficient reagent recycling present compelling advantages over more energy-intensive alternatives like steel slag carbonation. With China's coal-to-chemical industry generating 33 million tons of slag annually, this TRL 5-6 technology offers a practical pathway to transform waste liabilities into valuable resources while addressing climate emissions. Further optimization of the NH_4Cl pyrolysis conditions and aluminum precipitation pH (4.5-5.0) could enhance both the environmental and economic performance as the technology scales toward commercial implementation.

These studies reveal mineral carbonation's maturation from lab-scale curiosity to scalable climate technology, with two parallel trajectories: (1) feedstock diversification (high-Ca slags → low-Ca mining waste) and (2) process integration (pure CO_2 storage → circular resource recovery). Yet persistent gaps, energy optimization, byproduct management, and scale-up, underscore the need for the integrated LCA/TEA framework developed in this thesis (Chapters 3–4), which evaluates not just technical feasibility but systemic viability.

2.11 Process Performance Comparison

Mineral carbonation performance hinges on three interdependent factors: (1) feedstock reactivity (governed by composition and particle size), (2) process design (direct vs. indirect, reactor type), and (3) reaction conditions (T, P, additives). This section synthesizes laboratory-scale efficiencies across pathways, contextualizing their trade-offs for industrial deployment. This synthesis reviews the overall yield of mineral carbonation across different technologies, highlighting their advantages and challenges. For instance. mineralization of steel slag via several pathways showed that key factors effecting the overall process are the particle size of alkaline solid waste, the rotating speed of the rotary packed bed (RPB), the solid/liquid ratio, and the reaction temperature. Since the carbonation reaction is considered diffusion-controlled (i.e., limited by mass transfer), a rotating packed bed (RPB) reactor was introduced to enhance mass transfer between phases. This is achieved through its high centrifugal forces and excellent micro mixing capability [41]. Furthermore, the carbonation reaction can be enhanced by coupling with cold-rolling wastewater (CRW) due to its alkaline properties. Consequently, the CO_2 removal efficiency (i.e., the percentage of CO_2 removed from the emission source) using BOFS/CRW in the RPB process reached 96–99% with a retention time of less than one minute under ambient temperature and pressure conditions [41]. The high concentration of Na^+ and Cl^- in CRW might accelerate the leaching behavior of Ca-bearing phases in BOFS. This suggests that the leaching concentration of calcium ions in CRW should be higher than that in DIW, thereby resulting in a greater

carbonation reaction rate and higher CO_2 capture capacity.

In the carbonation of RCA, particle size significantly impacts the process. When CO_2 injection begins, RCA rapidly gains mass due to CO_2 absorption by pore water within the cement paste, which binds gravel and sand. This paste, rich in phases like portlandite and C-S-H, reacts with CO_2, forming bicarbonate and carbonate ions and precipitating $CaCO_3$. Calcium ions are progressively leached from cement minerals to sustain the reaction until calcium is depleted, at which point mineral dissolution slows. As carbonation progresses, CO_2 diffusion through carbonated layers becomes rate-limiting, reducing the mineralization rate. The continued CO_2 uptake in experiments indicates ongoing carbonation, though cement minerals have not yet fully carbonated.

Fine RCA material exhibits faster CO_2 uptake and can store more CO_2 per unit mass due to two key factors: its larger surface area, which enhances reaction rates, and its higher content of hydrated cement, resulting from the tendency of concrete to break along phase boundaries during crushing. All particle sizes mineralize CO_2, but smaller fractions contribute more significantly per mass, whereas larger particles, despite lower specific CO_2 uptake, contribute substantially due to their mass.

To determine the reaction yield of RCA carbonation, laboratory experiments based on Tiefenthaler, et al. indicate that the smallest size fraction achieves a reaction yield of 46%. Table 2.2 summarizes various mineralization pathways categorized based on the type of reactor or process, feedstock characteristics, and reaction conditions. These pathways are further classified as either direct or indirect carbonation processes. Direct carbonation pathways involve a single-step reaction where CO_2 directly reacts with the feedstock, typically under controlled temperature and pressure conditions. Examples include the CSTR (Continuously Stirred Tank Reactor) and RPB (Rotary Packed Bed) pathways, which use feedstocks like serpentine, olivine, or steel slag.

Indirect carbonation pathways break the reaction into multiple steps, extraction and carbonation. Abo Academy pathway and the Nottingham pathway, which use pretreatment methods like solid/solid or aqueous extraction to prepare the feedstock for carbonation.

The classification presented here aligns with the criteria described by Müller et al. [6] considering process design, feedstock preparation, and overall performance. This structure ensures clarity when comparing the advantages, disadvantages, and efficiencies of each pathway.

Table 2.3 Comparison of Mineralization Approaches by Feedstock and Performance

Mineralization Pathway	Concept	Heat pretreatment	Particle size (µm)	Pure CO2	temperature (°C)	yield (%)	Ref.
CSTR-115 bar (serpentine)	Aquous Direct	Yes	37	Yes,	185	92	[58]
CSTR-10 bar (serpentine)	Aqueous Direct	Yes	37	No	40	61	[58]
CSTR-150 bar (olivine)	Aqueous Direct	No	<10	Yes	185	81	[58]
AA Pathway (serpentine)	Indirect	Yes	75	Yes	510	78	[59]
Nottingham pathway (serpentine)	Indirect (PH swing)	No	75-150	No	80	87	[60]
RPB (steel slag)	Aqueous Direct	No	<125	No	25	96	[41]
Stirred batch (EAF)	Aqueous Direct	No	<150	Yes	50	50	[50]
Steel slag (Carbonic anhydrase bacteris)	Aqueous Direct	No	30-40	Yes	25	100	[61]
Fixed bed (RCA)	Gas-solid Direct	No	<65	Yes	25	95	[54]

3 Methodology

3.1 Research design

This study's research design seeks to explore and analyse two distinct carbon mineralizaion processes in Austria. The first process involves the utilization of biogenic CO_2 by mineralization with recycled concrete aggregates (RCA), while the second focuses on the carbonation of steel slag using process-generated CO_2, a byproduct from steel manufacturing facilities. The primary objective is to assess the feasibility of both process designs by applying life cycle assessment (LCA) and techno-economic analysis (TEA) to evaluate their environmental and economic impacts. Each process is driven by different underlying objectives and operational characteristics, which are examined to understand their respective benefits and challenges within the context of carbon mineralization. For the first process, the study incorporates a sensitivity analysis of the process chain, specifically focusing on the liquefaction and crushing unit operations, as these steps significantly influence overall performance. In addition, an economic sensitivity analysis is performed to assess the influence of RCA pricing and the market value of the value-added product on overall economic feasibility. The second process is evaluated in the conceptual design phase, with the goal of assessing its feasibility from both environmental and economic perspectives. A key component of this evaluation is a sensitivity analysis on the potential market prices of value-added materials produced during the process, as these can considerably affect its economic viability. Additionally, a sensitivity analysis is conducted to examine the environmental impacts associated with different electricity sources available in Austria, highlighting how the choice of energy supply influences the overall sustainability of the process. By integrating LCA and TEA with these targeted sensitivity analyses, the study aims to offer a detailed and comparative understanding of how each process functions, and to assess their implications for environmental sustainability and economic feasibility.

3.2 Utilization of biogenic CO_2 by mineralization with RCA

To assess the environmental and economic implications of CO_2 utilization, it is important to quantify the CO_2 generated as a byproduct by biogas upgrading facilities in Austria. Table 3.1 presents this data, which has been collected directly from plant websites or through direct contact with the facilities. This information provides a basis for further analysis of CO_2 capture and utilization strategies discussed in this thesis.

Table 3.1: Annual CO_2 Emissions from Biogas Plants

Biogas plant	Annual CO_2 Emission (kton/year)
Bruck a. d. Leitha	3.96
EVN	5.96
Engerwitzdorf	1.14
Häusle	3.40
Reitbach	1.89
Steindorf	1.71
Zemka	1.59
Pfaffenau	1.20
Wiener Neustadt süd	1.31
Steiermark	0.95
11er Nahrungsmittel	4.21

The process of utilizing biogenic CO_2 for mineralization with RCA involves several stages aimed at maximizing the efficiency of carbon capture and subsequent mineralization efforts. Initially, biogenic CO_2 is liquefied to facilitate its transportation to designated RCA sites, where it undergoes a controlled phase change back to the gaseous state using an evaporator system. This preparation phase ensures the CO_2 is in an optimal state for subsequent reactions. Once on-site, the gaseous CO_2 is integrated into the mineralization process with concrete waste materials. The systematic approach of liquefying, transporting, evaporating, and integrating biogenic CO_2 into concrete waste mineralization underscores a method to enhance environmental sustainability. By effectively utilizing biogenic CO_2 in conjunction with RCA, this process contributes to mitigating greenhouse gas emissions while simultaneously addressing waste management challenges within the construction industry. RCA undergoes also a preparation phase designed to optimize its reactivity with CO_2. This process begins with the utilization of a crusher; by decreasing particle sizes, the surface area of the concrete waste is effectively increased, thereby creating more available sites for the absorption and subsequent mineralization.

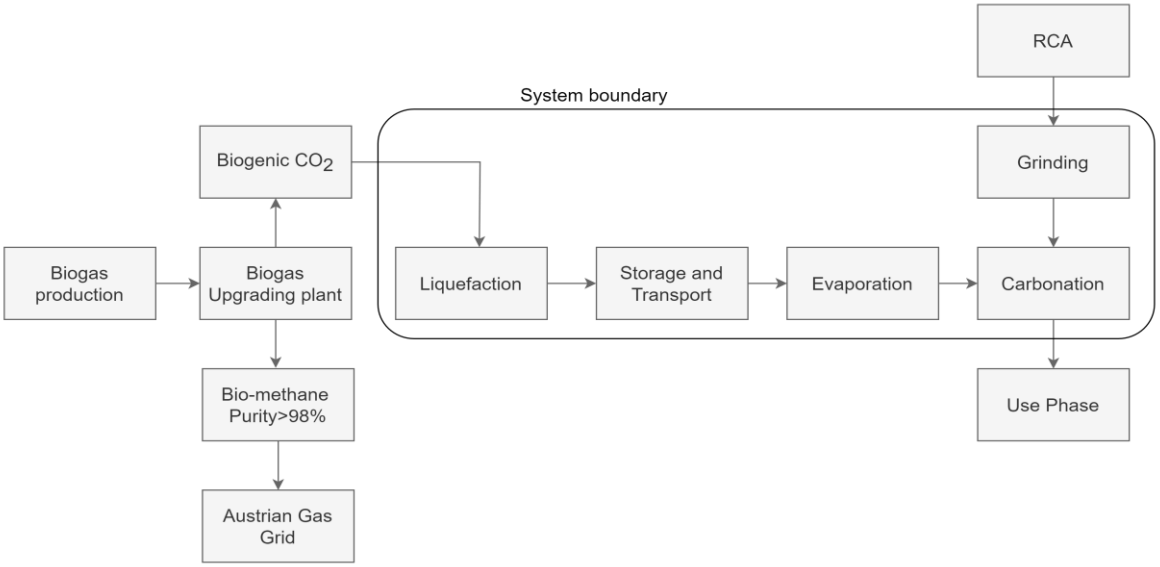

Fig. 3.1 RCA Carbonation via Biogas upgrading CO_2

Biogas primarily consists of methane (CH_4) in concentrations ranging from 50% to 70% and carbon dioxide (CO_2) at concentrations of 30% to 50%. This composition can vary depending on the type of organic material used and the specific conditions of the anaerobic digestion (AD) process (mainly dependent on the nature of the substrate and pH of the reactor) [62]. Besides these two gases, biogas additionally contain minor amounts of other compounds. High methane content in biogas makes it a valuable renewable energy source, while the carbon dioxide component must often be removed to improve the quality and usability of the biogas.

Table 3.2: Chemical Composition of Biogas [62]

Compounds	Concentration range	Unit
CH_4	50-70	%Vol
CO_2	30-50	%Vol
N_2	0-3	%Vol
H_2O	5-10	%Vol
O_2	0-1	%Vol
H_2S	0-10000	ppm
NH_3	0-100	ppm
hydrocarbons	0-200	mg/m^3
siloxanes	0-41	mg/m^3

The energy content of methane described by the Lower Calorific Value (LCV) is 50.4 MJ/kg CH_4 or 36 MJ/m^3 CH_4 (at STP conditions) [63]. Therefore, it is well understood that the higher the CO_2 or N_2 content is, the lower the LCV in biogas. For biogas with methane

content in the range of 60–65% the LCV is approximately 20–25 MJ/m^3 biogas. This upgrading process typically removes impurities such as CO_2, water vapor, hydrogen sulphide (H_2S), and other trace gases to enhance the quality and energy content of the biomethane. Biomethane production not only yields a renewable energy source but also offers environmental benefits by diverting organic waste from landfills, reducing methane emissions, and providing a sustainable alternative to fossil fuels. By integrating waste management with renewable energy generation, biomethane production exemplifies a closed-loop approach that contributes to both energy security and environmental stewardship. For the purposes of Life Cycle Assessment (LCA) and Techno-Economic Analysis (TEA) in this research, several key assumptions are made regarding the biogas composition and treatment processes. It is assumed that the biogas consists of 40% CO_2 and 60% methane (CH_4). Additionally, apart from liquefaction, no further preparation of CO_2 is required for its transportation to the concrete waste plant. To facilitate the calculations, it is assumed that the lower calorific value (LCV) of biogas is 20 MJ/m^3. This value is essential for determining the CO_2 quantity when biogas upgrading systems report production in terms of calorific values. Further assumptions include the separate CO_2 having a temperature of 40°C and being at atmospheric pressure.

3.2.1 Liquefaction of CO_2

A critical component of CCU processes is the efficient and safe transportation of CO_2 from its sources to designated sinks. Ensuring cost-effective transportation methods will be crucial for the practical and widespread adoption of CCU strategies. Different liquefaction technologies, such as cryogenic cooling, compression, or absorption processes, each have unique energy requirements, costs, and environmental footprints. The choice of technology can significantly influence the efficiency and sustainability of the entire CO_2 utilization process. Therefore, a thorough life cycle assessment (LCA) and techno-economic analysis (TEA) of the liquefaction options must be conducted. By integrating these considerations into the planning and implementation phases, the mineralization value chain can be optimized, enhancing the overall feasibility and effectiveness of carbon capture and utilization strategies. This evaluation ensures that the chosen method not only meets technical requirements but also aligns with broader sustainability goals.

the present work adopts a dedicated thermodynamic modelling approach to systematically evaluate the liquefaction process. The model, illustrated in Fig.3.2, was developed independently through manual thermodynamic analysis, ensuring transparency and adaptability

to mineralization process requirements. The primary objective of this analysis is threefold: first, to quantify the pressure-dependent energy consumption and material utilization (e.g., stainless steel) of the liquefaction process; second, to integrate these findings into a comprehensive life cycle assessment (LCA) and techno-economic analysis (TEA) framework; and third, to identify the optimal delivery pressure that maximizes the overall efficiency of the subsequent carbonation process.

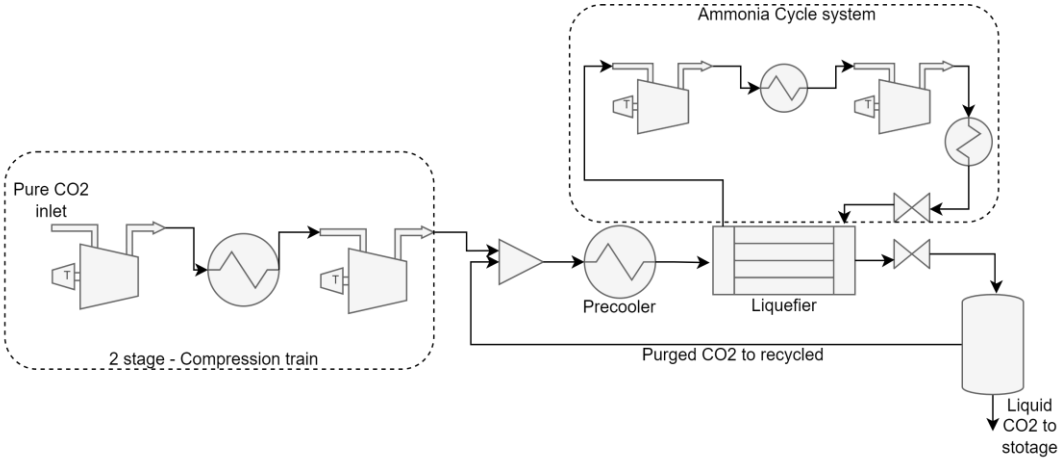

Fig. 3.2 Ammonia-Cycle liquefaction system layout with 2 stage-Compression train

For the compression stages, an isentropic efficiency (η_{is}) of 85% was assumed, which is typical for compression systems [64]. To begin, the maximum compression ratio for each stage is set at 3, which is used to determine the intermediate pressures and temperatures. The relationship between temperature and pressure for an isentropic process is utilized to compute the temperature after each compression stage.

$$\frac{T_{out}}{T_{in}} = \left(\frac{P_{out}}{P_{in}}\right)^{\frac{\gamma-1}{\gamma}} \tag{3.1}$$

Where T_{in} is the temperature before compression (reset to 40°C or 313.15 K after intercooling), γ is the heat capacity ratio (approximately 1.3 for CO_2), and P_{in} and P_{out} are the pressures before and after each stage of compression. For each stage, the isentropic work required for compression is calculated using Eq. (3.2) [64]. Since real compressors are not perfectly isentropic, the real work required is adjusted by the isentropic efficiency (see Eq. (3.3)).

$$W_{is} = \frac{\dot{m}RT_{in}}{\gamma-1}\left[\left(\frac{P_{out}}{P_{in}}\right)^{\frac{\gamma-1}{\gamma}} - 1\right] \tag{3.2}$$

$$W_{real} = \frac{W_{is}}{\eta_{is}} \quad (3.3)$$

Where:

- $\dot{m}$(kg/s) is the mass flow rate
- R is the specific gas constant for CO_2 approximately 188.9 (J/kg·K) and for NH_3 is 488 (J/kg·K) [65].
- W_{is} , W_{real} are the isentropic and real work (J/s)

Heat exchangers are modelled using counter-current flow configurations. To assess the design and performance of a heat exchanger, it is essential to define the inlet and outlet parameters for both fluid streams. The cooling duty of the heat exchanger can be determined based on the characteristics of the hot stream, the CO_2 stream. However, because the specific heat capacity Cp($J.kg^{-1}K^{-1}$) varies with temperature for a given delivery CO_2 pressure, calculating the heat duty for intercooling units in a compression train requires accounting for these variations [63]. For accurate determination, the heat duty is calculated based on the outlet temperature (T_{out}) and pressure (P_{out}) of each compression stage. The intercooler reduces the CO_2 stream temperature back to 40°C after each compression stage, Lowering the temperature further using water-based intercooling would require significantly larger heat exchangers and increased cooling water flow rates, potentially exceeding practical limits. Lower temperatures (e.g., 30°C) could reduce liquefier load but require prohibitive cooling water volumes. As illustrated in Fig. 3.2, following the final stage of compression and preceding the liquefier, which utilizes ammonia as a coolant, the temperature is reduced to 40°C in a precooler. This cooling step is implemented to minimize the thermal load on the liquefier, thereby facilitating the achievement of the final desired temperature more efficiently. To calculate the cooling duty of a liquefier, it is essential to follow an approach that considers both sensible and latent heat requirements (see Eqs. (3.4), (3.5), (3.6)). The process begins by defining the inlet and outlet conditions of the gas. The calculation assumes that the liquefier operates isobarically, meaning that the inlet and outlet pressures (P_{in} and P_{out}) are the same as the pressure achieved in the compression train. Additionally, it is assumed that there is no pressure drop across the heat exchangers, including the intercooler, precooler, and liquefier.

$$Q_{total} = Q_{cooling} + Q_{phase} \quad (3.4)$$

$$Q_{cooling} = \dot{m}.C_p.\Delta T \quad (3.5)$$

$$Q_{phase} = \dot{m}.h_{fg} \quad (3.6)$$

Where:

- Q_{total} (J/s) is the total heat
- $Q_{cooling}$ (J/s) is the sensible heat
- Q_{phase} (J/s) is the latent heat during phase change
- $\dot{m}$(kg/s) is the mass flow rate of CO_2
- Cp (J/kg·K) is the specific heat capacity of CO_2 at constant pressure
- ΔT (K) is the temperature change during cooling
- h_{fg} (J/kg) is the latent heat of vaporization (or condensation)

To accurately calculate the latent cooling demand, it is essential to consider the dew point temperature of CO_2 at different delivery pressures. The dew point temperature indicates where CO_2 begins to condense and is crucial for determining the amount of heat that must be removed to convert the gas to a liquid. Table 3.1 summarizes the calculated work and cooling duty requirements for liquefying CO_2 at 0.1 kg/s (Base case) across different delivery pressures (using Eqs 3.1–3.6). The results highlight the influence of pressure on compression work and cooling loads.

Table 3.3: Cooling Duty and Compression Work at different Pressures (0.1 kg/s Flow Rate)

Pressure (bar)	Cooling Duty (kw)		Compression Work (kw)					
	CO_2 intercooling	Liquefier	NH3-Cycle	1st stage	2nd stage	3rd stage	4th stage	NH_3(2 stages)
7	14.94	42.94	7.17	6.7	5.02	0	0	6.23
10	17.97	41.62	6.95	6.7	6.7	0.57	0	6.04
15	21.02	37.65	6.29	6.7	6.7	2.91	0	5.47
20	23.47	35.18	5.87	6.7	6.7	4.7	0	5.11
25	25.67	32.90	5.49	6.7	6.7	6.17	0	4.78
30	27.31	30.70	5.13	6.7	6.7	6.7	0.57	4.46
40	29.81	26.95	4.50	6.7	6.7	6.7	2.20	3.91
50	31.98	23.19	3.87	6.7	6.7	6.7	3.55	3.37
60	33.95	19.74	3.30	6.7	6.7	6.7	4.70	2.87
70	35.72	18.40	3.03	6.7	6.7	6.7	5.71	2.67

This table presents the base case work and cooling requirements at various CO_2 delivery pressures for different plant configurations. The data serves as the foundation for both the

life cycle assessment (LCA) and techno economic analysis (TEA) carried out in this thesis.

3.2.2 Weight estimation model for compressors

This study adopts a semi-empirical power-law correlation (see Eq. (3.7)) to estimate compressor weight as a function of power input, based on scaling principles discussed in centrifugal compressors (Boyce et. al. [66]).

$$W = C.P^{n} \quad (3.7)$$

Where:

- W= Estimated weight (kg)
- P= Power input (kW)
- C, n = Empirical constant (with C=70, n=0.6)

The exponent "n" was estimated based on observed non-linear trends in weight to power ratios across compressor datasheets. The constant "C" reflects typical construction materials and thermal resistance in standard gas compression systems. Parameter values were independently defined using technical assumptions based on vendor data.

The compression work for different delivery pressures at 0.1 kg/s are presented in table 3.3 and based on them the weight estimation for different compression stages including CO_2 compression stages and Compressors in NH_3 Cycle are provided in Table 3.4

Table 3.4: Compressor Weight Estimation for 0.1 kg/s Flow

Pressure (bar)	Compressor's weight estimation (kg)				
	1st stage	2nd stage	3rd stage	4th stage	NH_3 (2stages)
7	219.2	184.2	0	0	209.08
10	219.2	219.2	50.07	0	205.9
15	219.2	219.2	132.7	0	193.9
20	219.2	219.2	177.1	0	186.2
25	219.2	219.2	208.7	0	178.9
30	219.2	219.2	219.2	50.01	171.6
40	219.2	219.2	219.2	112.5	158.7
50	219.2	219.2	219.2	149.7	145
60	219.2	219.2	219.2	177.1	131.6
70	219.2	219.2	219.2	199	126

3.2.3 Weight estimation model for heat exchangers and liquefiers

Estimation of the heat exchanger weight by linking it to heat duty (Q), heat transfer area (A), and material properties:

$$W = \rho_m . t. \left(\frac{Q}{U.\Delta T_m}\right) \quad (3.8)$$

Where:

- W= Estimated weight (kg)
- ρ_m= Material density (kg/m^3)
- t = Effective wall thickness (m)
- Q = Heat duty (W)
- U = Overall heat transfer coefficient (W/m^2.K)
- ΔT_m= Log mean temperature difference (K)

For preliminary analysis, fixed overall heat transfer coefficients (U) are assumed: 2000 W/m²K for liquefier (CO_2/NH_3), 800 W/m^{2}K for NH_3/water-glycol systems, and 500 W/m^{2}K for gas-liquid intercoolers. These values account for typical performance ranges while simplifying initial calculations. A constant ΔT_m of 10 °C is assumed for all cases. All heat exchangers in this study are assumed to be constructed from 18/8 chromium steel, representing a conservative approach that may overestimate the weight of compact liquefiers, while ensuring corrosion resistance under all operating conditions.

3.2.4 Storage and transport

The design of liquefied CO_2 storage and transportation tanks requires consideration of pressure levels and weight estimation. This methodology follows the principles outlined in design of vertical pressure Vessel (Yahya et al. [67]), adapting the equations for shell and head thickness calculations for different pressures (7–70 bar). The system is designed for a CO_2 liquefaction rate of 0.1 kg/s. The selected material is stainless steel (18/8 chromium-nickel steel), A corrosion allowance of 3 mm is applied, and the design temperature range is set between -50°C and 30°C to account for liquefaction conditions. The shell thickness for each pressure vessel is calculated using Eq. (3.9).

$$t_s = \frac{P.r}{S.E - 0.6P} + C_{corr} \quad (3.9)$$

Where:

- t_s= Shell thickness

- P = Design pressure (MPa)
- r =Inner radius (mm)
- S = Allowable stress
- E = Weld joint efficiency (1.0 for fully radiographed welds)
- C_{corr} = Corrosion allowance (3 mm)

For the heads, the required thickness is determined by:

$$t_h = \frac{P.d}{2S.E - 0.2P} + C_{corr} \quad (3.10)$$

Where:

- d = inner diameter (mm)

The allowable stress for chromium-nickel steel is assumed 118 MPa [67], with a material density of 8,000 kg/m³ for stainless steels [68]. The base tank configuration uses reference dimensions of 1.0 m internal diameter and 2.0 m cylindrical length; Dimensions are proportionally scaled to achieve the exact 360 kg capacity at each pressure level while preserving geometric ratios. Tank weights are calculated through Eqs. (3.10),(3.11).

$$W_{shell} = \pi . L . \rho . ((r + t_s)^2 - r^2) \quad (3.11)$$

$$W_{head} = \frac{4}{3} \pi . \rho . ((r + t_h)^3 - r^3) \quad (3.12)$$

The calculated weights for all pressure levels (7–70 bar) are summarized in Table 3.5 demonstrating how higher pressures necessitate thicker walls and larger dimensions to maintain the 360 kg CO_2 capacity, ultimately increasing total tank mass.

Table 3.5: CO_2 Tank weight estimation

Pressure (bar)	Temperature (C)	CO_2 density (kg/m3)	Tank weight (kg)
7	-55	708	680
10	-45	696	730
15	-34	683	780
20	-25	672	870
25	-17	662	960
30	-11	655	1050
40	0	641	1180
50	9	629	1310
60	17	619	1440
70	20	620	1570

The average transportation distance from plants to concrete facilities, located across various regions, is 20 kilometers. The transport vehicle has a gross weight of 7.5 tons and carries up to 1 ton of CO_2. For this study, it is assumed that the delivery temperature is consistently 5 degrees Celsius lower than the saturated temperature for each specified pressure.

3.2.5 Evaporation

The evaporator's thermal energy requirement was evaluated across a range of initial pressures (7–70 bar), as documented in Table 3.5, where liquefied CO_2 enters at saturation conditions and exits as a gas at 1 bar and 25°C. The total thermal duty is calculated by combining the latent and sensible heat contributions. Both are based on enthalpy changes:

$$Q_{total} = \Delta h_{latent} + \Delta h_{sensible} \quad (3.13)$$

Here, Δh_{latent} is the enthalpy change for vaporization at the initial pressure, and $\Delta h_{sensible}$ is the enthalpy change for heating and depressurizing the vapor to the final conditions (1 bar, 25°C). This approach accounts for both phase change and pressure effects. Table 3.6 presents the total thermal duty required for the evaporation of liquefied CO_2 at different initial pressures, calculated for a fixed mass flow rate of 0.1 kg/s.

Table 3.6: CO_2 evaporation duty at various pressures

CO_2 delivery pressure (bar)	Thermal duty (kW)
7	41.2
10	39.3
15	36.9
20	35
25	33.4
30	31.9
40	29.2
50	26.8
60	24.3
70	21.2

3.2.6 Carbonation

The mineralization plant setup from Tiefenthaler et al. [54] is adapted for the carbonation of RCA with different particle sizes. The approach assumes that the scaling of the miner-

alization low-alloyed steel containers follows a sub linear relationship with respect to capacity, proportional to the 0.6 power of the scaling factor, while the power output scales linearly. The CO_2 flow rate is set at 0.1 kg/s for the process (base case), calculated based on the expected reaction rate and carbonation capacity. This flow rate is considered constant for all particle sizes, though variations in particle size may affect the mineralization efficiency. To provide transparency, table 3.7 shows the calculations and assumptions used for scaling the mineralization process for RCA with different particle sizes. This includes the weight of containers, power requirements, and CO_2 storage efficiency for each scenario.

Table 3.7: Scaling parameters for RCA Carbonator at 0.1 kg/s CO_2

	RCA Size fractions (mm)						
	0-0.064	0.065-0.125	0.125-0.250	0.250-0.5	0.5-1.0	1.0-2.0	2.0-4.0
CO_2 uptake/ ton RCA	48	32	28	21	15	12	11
Carbonated RCA (ton/day)	162.5	243.8	278.6	371.4	520	650	709.1
Carbonator weight (ton)	16.07	20.50	22.21	26.36	32.30	36.93	38.91
Power (kW)	2.71	4.06	4.64	6.19	8.67	10.83	11.82

3.2.7 Crushing of RCA

According to Tiefenthaler et al. [53], the particle size distribution of Recycled Concrete Aggregate (RCA) plays a crucial role in influencing CO_2 uptake during the carbonation process. This impact is significant because it directly affects the efficiency of calcium carbonate ($CaCO_3$) production for a given quantity of RCA. Consequently, variations in particle size can alter the number of mineralization containers required (as discussed in previous section) for optimal operation. In this context, the Bond equation is commonly employed to calculate the energy required for the crushing of RCA [69], which is a key factor in determining the optimal particle size distribution.

$$W_m = 10\, W_i \left(\sqrt{\frac{1}{d_{80,\omega}}} - \sqrt{\frac{1}{d_{80,\propto}}} \right) \text{ (bond equation)} \qquad (3.8)$$

Where:

W_m= mass-related energy requirement for crushing (kWh/ton)

W_i = Bond work index

$d_{80,\omega}$ = Particle size of the crushed product

$d_{80,\propto}$ = Particle size of the feed material

Given these considerations, one of the primary objectives of this study is to identify the most effective particle size distribution. This will be achieved through a comprehensive analysis using Life Cycle Assessment (LCA) and Techno-Economic Analysis (TEA). For the base case, designed to mineralize a CO_2 flow rate of 0.1 kg/s, the energy requirement for RCA crushing is calculated using the Bond equation, considering different target particle sizes. To estimate the weight of the crushing machinery corresponding to different capacity demands, technical data from the JXSC Mine Machinery data sheet [70] is used as a reference.

Table 3.8: RCA Size Impact at 0.1 kg/s CO_2

	RCA Size fractions (mm)						
	0-0.064	0.065-0.125	0.125-0.250	0.250-0.5	0.5-1.0	1.0-2.0	2.0-4.0
CO_2 uptake ($kgCO_2$/ ton RCA)	48	32	28	21	15	12	11
Annual CO_2 input (ton / year)	2,880	2,880	2,880	2,880	2,880	2,880	2,880
Annual RCA Requirement (ton/year)	60,000	90,000	102,857	137,142	192,000	240,000	261,818
RCA flow rate (ton/hour)	7.5	11.3	12.9	17.1	24.0	30	32.7
Specific crushing energy (kWh/ton RCA)	15.5	10.7	7.2	4.7	2.9	1.7	0.8
Hourly crushing energy demand (kWh)	116.5	120.6	92.6	80.6	69.6	51	25.5
Weight of crusher (ton)	24.5	31.2	33.9	40.2	49.2	56.3	59.3

Table 3.8 summarizes the impact of RCA particle size on CO_2 uptake efficiency, material demand, energy consumption, and crusher sizing, assuming an annual CO_2 input of 2,880

tons (corresponding to a continuous flow rate of 0.1 kg/s). Finer RCA fractions, such as 0–0.064 mm, exhibit the highest CO_2 uptake (48 kg CO_2/ton), while coarser fractions like 2.0–4.0 mm achieve only 11 kg CO_2/ton. As a result, the total annual RCA requirement increases with particle size, from 60,000 tons for the finest to over 261,800 tons for the coarsest material. This increase in material throughput also affects the hourly processing rate, which grows from 7.5 to 32.7 tons/hour across the size range. Specific crushing energy demand decreases with larger particle sizes (from 15.5 to 0.8 kWh/ton), leading to lower total energy input per hour. However, due to the higher mass flow, the size and weight of the crusher still increase, rising from 24.5 to 59.3 tons. These findings underline a key trade-off: finer RCA enables higher CO_2 capture per ton but requires more energy-intensive processing and lower-throughput equipment. In contrast, coarser RCA reduces the energy per ton but increases the overall mass throughput and requires larger crushing units.

3.2.8 Mass and Energy Balance for RCA Carbonation Process at 0.1 kg/s CO_2

In this study, the CO_2 mineralization process was modeled based on industrial conditions from Tiefenthaler et al. [54], assuming ambient temperature (25 °C), atmospheric pressure in the reactor, CO_2 delivery pressure of 60 bar, RCA size fraction of 2–4 mm, and a CO_2 conversion rate of 95%. For a continuous CO_2 flow of 0.1 kg/s (360 kg/h), a one-hour mass and energy balance were established. The balance includes 32.7 tons of RCA and 360 kg CO_2 as inputs, with 342 kg CO_2 converted to 777.3 kg $CaCO_3$, ~435.3 kg RCA consumed, and 18 kg CO_2 unreacted. Energy inputs were estimated using the methodology described in the previous sections, covering CO_2 liquefaction, transport, evaporation, carbonation, and RCA crushing. Fig. 3.3 summarizes the mass balance.

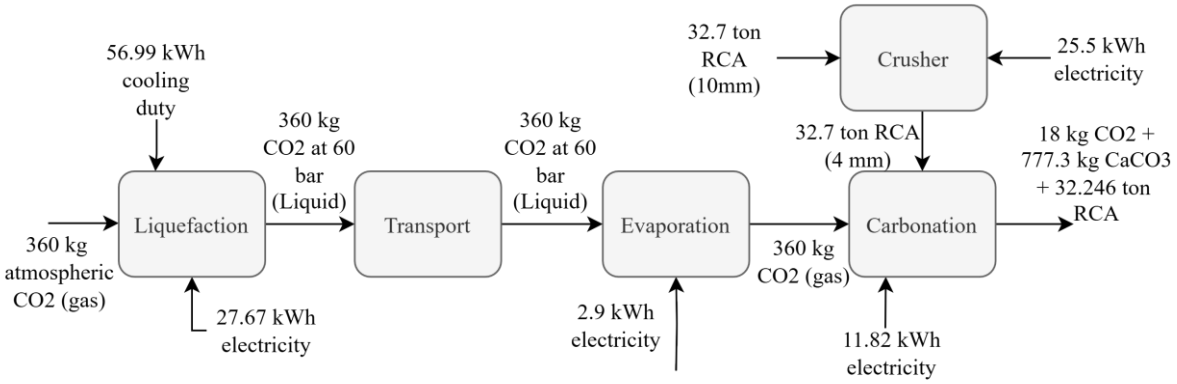

Fig. 3.3 Mass balance of RCA carbonation (0.1 kg/s CO_2, 60 bar, 2–4 mm)

3.3 Carbonation of Steel Slag using Process- Generated CO_2

This case, a share CO_2 emission from steel production is captured and used to carbonate the steel slag, as the amount of the steel slag is limited, which can then potentially be reintroduced into the production process or used in other beneficial ways. This approach aims to minimize waste and maximize resource efficiency within the steel production process. To begin evaluating the potential of this approach, it is initially conducted a comprehensive review of CO_2 emission data related to steel production processes in Austria. This data was obtained from reports in the Austrian emission trading registry [71].

Table 3.9: Chemical Composition (%) of Steel Slag [72],[73]

Slag type	Chemical composition (%)					
	CaO	MgO	Al_2O_3	SiO_2	Fe_2O_3	Others
BF&BOF	42	8	7	23	11	9
EAF	38	6	6	28	15	7

As Rawlins et al [74] demonstrated, the slag production rates associated with different steel production technologies are as follows: for Electric Arc Furnace (EAF) technology, the slag generation is 0.08 kg of slag per kg of steel, whereas for Basic Oxygen Furnace (BOF) technology, it is 0.15 kg of slag per kg of steel. A summary of the data collected from five steelmaking factories in Austria is presented in the Table 3.10.

Table 3.10: Steel Plant CO_2 Emissions and Steel Slag Production

Plant name	By- Products	
	CO_2 Emissions (kton)	Steel Slag (kton)
Stahlwerk Marienhütte GmbH	37.6	25
Stahlproduktion Kapfenberg	127.6	85.8
Voestalpine Linz	8,880.7	2566.7
Voestalpine Donawitz	2,784.6	804.8
Edelstahl Mitterdorf	21.1	14.2

3.3.1 Process Layout

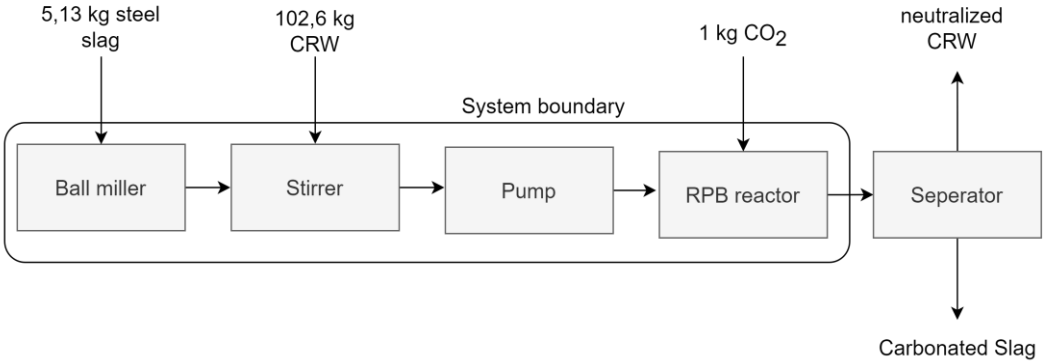

Fig. 3.4 Process layout of steel slag carbonation

The aim of this part of this thesis is an evaluation of the feasibility of scaling up a specific process from the laboratory scale to industrial-scale operations. This process involves capturing CO_2 through a combination of leaching and carbonation techniques applied to alkaline steelmaking waste. The core technology is the use of a rotating packed bed (RPB), which is designed to enhance the efficiency of gas-liquid interactions, thus improving the effectiveness of CO_2 capture. Figure 3.4 illustrates the layout of the process, beginning with the leaching of alkaline steelmaking slag to extract reactive ions. The resulting solution or slurry is then introduced into the rotating packed bed (RPB), where it reacts with CO_2 in a carbonation process to capture the carbon dioxide effectively.

3.3.2 Ball mill

The energy requirement for the crushing of steel slag is calculated using the Bond equation (see Eq.3.8), as previously presented. The estimation focuses on the reduction of particle size from 10 mm to 125 µm, assuming a Bond work Index of 12 kWh/ton. This energy requirement is derived for a base case scenario involving a throughput of 513 kg of steel slag per hour, which corresponds to the amount of slag required to mineralize 100 kg of CO_2. The resulting energy consumption for this specific size reduction is 9.53 kWh/ton, equating to a total energy demand of annually 39,124 kWh of crushing operation. The equipment weight for this base case is estimated to be 4.6 tons, based on a crusher with a processing capacity of 513 kg/h [70], and is assumed to be constructed from low-alloyed steel for the purpose of the life cycle assessment. This value serves as the reference for scaling both energy demand and equipment weight across different plant scenarios using appropriate scaling relationships.

Table 3.11: Crushing parameters (100 kg/h CO_2)

Parameter	Value
CO_2 input rate (kg/h)	100
Steel Slag crushing rate (kg/h)	513
Annually energy demand (kWh)	39,124
Annually sequestrated CO_2 (kg)	800,000
Equipment weight (ton)	4,6

3.3.3 Leaching tank (stirrer)

As demonstrated by Shu-Yuan Pan [41], the leaching process for extracting different metal cations from steel slag achieves nearly 100% efficiency within one hour of leaching. Consequently, data for the leaching times are based on the optimal one-hour leaching duration. Due to varying capacities across different plants, a reference case is defined using a stirred leaching tank with a capacity of 72 m^3, a motor power of 7 kW, and a total equipment weight of 11 tons [70], and it is assumed to be constructed from chromium steel. Energy demand is assumed to scale linearly with capacity, while equipment weight is estimated using the six-tenths rule. The corresponding data for this base case are summarized in Table 3.12.

Table 3.12: Leaching tank base case indicators (100 kg/h CO_2)

Parameter	Value
Slurry flow rate (kg/h)	10,700
Motor power (kW)	1.04
Annually energy consumption (kWh/year)	8,320
Annually sequestrated CO_2 (kg)	800,000
Equipment weight (ton)	3,50

3.3.4 Pumping

In the process design for CO_2 mineralization using steel slag, slurry is pumped to facilitate the carbonation reaction. The slurry consists of water and steel slag, with an assumed density of approximately 1035 kg/m^3. To estimate the energy consumption of the slurry pump, a linear relationship is assumed between the pumping power and the flow rate. This assumption holds under the condition that the head (pressure), slurry density, and pump efficiency remain constant. The power required to pump the slurry is calculated using Eq. 3.9.

$$P = \frac{\rho.g.Q.H}{1000.\eta} \quad (3.9)$$

Where:

- P = power (kW)
- ρ = slurry density (1035 kg/m³)
- g = acceleration due to gravity (9.81 m/s²)
- Q = slurry flow rate (m³/s)
- H = total head (m)
- η = pump efficiency

For this analysis, the total head (H) is assumed to be 10 meters, and the pump efficiency (η) is set at 70%. To estimate the equipment mass associated with pumping, it is assumed that a slurry pump capable of delivering 5 m³/h has a weight of 150 kg [70], constructed from 18/8 chromium stainless steel. Given that each plant requires a different slurry flow rate, the six-tenths scaling rule is applied to determine the corresponding pump weight per functional unit for each case:

$$\text{Weight} = 150 \times \left(\frac{Flow_{new}}{5}\right)^{0.6}$$

Table 3.13: Pumping unit base data indicators (100 kg CO_2)

Parameter	Value
Slurry flow rate (kg/h)	10,700
Pump power	0.43
Annually energy consumption (kWh/year)	3,448
Pump weight (kg)	150

3.3.5 Rotating Packed Bed (reactor)

In the process design, the Rotating Packed Bed (RPB) will serve as a critical unit operation for enhancing CO_2 capture efficiency. The RPB is specifically chosen for its ability to improve gas-liquid interactions through its unique rotational motion, which significantly boosts the effectiveness of the carbonation process. The RPB units utilized in this design are sourced from [75], and their specifications are as follows: 150 m^3/h liquid and up to 5000 m^3/h gas flow, power during the operation 3 kWh and weight of 900 kg stainless steel.

Table 3.14: Rotating packed bed base data indicators (100 CO_2 kg/h)

Parameter	Value
Slurry throughput capacity (kg/h)	10,700
CO_2 sequestration rate (kg/h)	100
Power (kW)	2.14
Annually energy consumption (kWh/year)	17,120
RPB weight (kg)	734

3.3.6 Mass and Energy Balance for Steel Slag Carbonation Process (Base Case)

This section presented the modeling and calculation of the mass and energy balance for the steel slag carbonation process, based on a CO_2 conversion rate of 96% reported in the literature. The calculations for the base case of 100 kg/h CO_2 input, performed and explained in this chapter, show the formation of 218.2 kg $CaCO_3$. The results are summarized in Fig. 3.6 and provide a basis for assessing process performance.

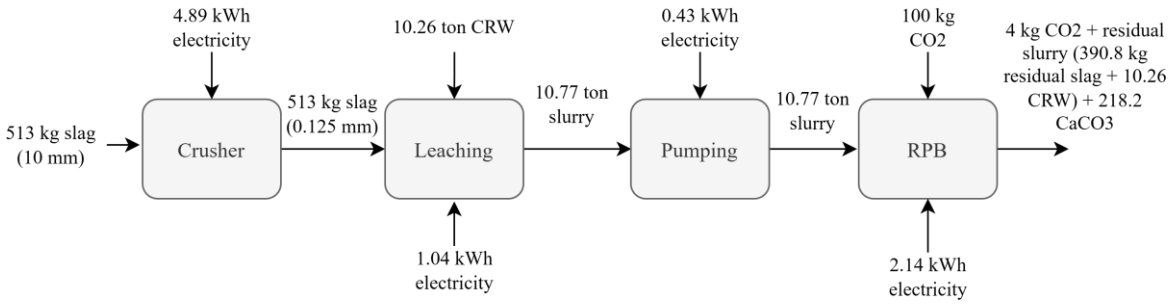

Fig. 3.5 Mass balance of steel slag carbonation (100 kg/h CO_2, 96% conversion)

3.4 Life Cycle Assessment (LCA)

The Life Cycle Assessment (LCA) methodology employed in this study adheres to the ISO 14040 and ISO 14044 standards [76]. The primary objective is to evaluate the environmental impacts associated with two distinct process designs.

3.4.1 Goal and Scope

The goal of this LCA is to independently evaluate the environmental impacts of:

- The mineralization of biogenic CO_2, focusing on the effects of different RCA size fractions and varying conditions of liquefied CO_2.

- The feasibility of carbonation of steel slag using CO_2 generated from the same processes.

These two processes are assessed in parallel, and while they are not compared directly, the findings for biogenic CO_2 mineralization under different conditions may be compared within its own context. Given the defined system boundaries, both assessments are characterized as 'gate-to-gate' LCAs, focusing exclusively on the environmental impacts within the specific processes of mineralization and carbonation, without accounting for upstream or downstream life cycle stages. For the mineralization of biogenic CO_2, the system boundaries encompass the entire mineralization process. Biogenic CO_2 is considered emission-neutral because it originates from vegetation, which has absorbed an equivalent amount of CO_2 from the atmosphere during its growth [77]. This CO_2 is released back into the atmosphere when the vegetation decomposes or is processed. The scope does not cover the production and upgrading of biogas, including the associated raw materials, energy, and impacts. Additionally, the lifecycle impacts of RCA production before its use in the mineralization process are not considered. The purification of CO_2 is also excluded, as it is assumed to be already in a pure state. For the RCA carbonation process, the RCA material itself is treated as a waste material and carries no environmental burden in the LCA; only its preparation steps (such as crushing) are considered. Similarly, for the steel slag carbonation process, the steel slag and CRW are considered waste and are not counted as inputs; only their preparation (e.g., grinding) and the energy required for stirring are included in the system boundaries. For the carbonation of steel slag using process-generated CO_2, the scope encompasses the carbonation process in which CO_2 generated during the process is utilized. This includes evaluating the environmental impacts associated with both the use of CO_2 and the processing of steel slag. The assessment does not cover the lifecycle impacts of steel slag production prior to its use in the carbonation process.

3.4.2 Functional Unit

The functional unit for both process designs is defined as **"1 kg of CO_2 mineralized"**. This common functional unit allows for a consistent basis to evaluate and compare the environmental impacts associated with the different processes under consideration. Specifically, for the CO_2 mineralization process, this unit measures the amount of CO_2 successfully mineralized.

3.4.3 Life Cycle Inventory (LCI)

The Life Cycle Inventory (LCI) in this study integrates both primary and secondary data sources. Emissions data were directly obtained from the participating plants and supplemented with calculated estimates where necessary. Power requirements were estimated using calculations informed by literature data and scaling approaches from analogous systems. Weight estimations for construction materials were derived from engineering calculations and validated with secondary data from the Ecoinvent database (accessed via Activity Browser v. 2.9.0). Ecoinvent datasets were also utilized to quantify the carbon footprint associated with activities related to the carbonation processes, as detailed in Table A.1 (see Appendix).

3.4.4 Steel Recycling and loss quantification framework

This study employed the MacTrace Global model to analyze steel recycling flows and losses across multiple life cycles and regions. The methodology integrated dynamic stock modeling with trade pattern analysis to track steel through production, use, and recovery phases. Key loss mechanisms were systematically quantified, including remelting losses (5% as slag/dust), incomplete scrap recovery from end-of-life products, dissipation through corrosion and unrecovered obsolete stocks, and quality losses from downcycling into lower-grade applications. The High Recovery scenario (95% fabrication yield, 95% end-of-life recovery, 97% remelting yield) was analyzed to assess optimized recovery potential. The model incorporated regional variations in recovery efficiencies and explicitly accounted for how global trade redistributes scrap materials, potentially exacerbating losses when exported to regions with less efficient recycling infrastructure. Scenario analyses examined how technological improvements and policy interventions could mitigate these losses while maintaining material functionality (Pauliuk et al. [78]).

3.4.5 Impact assessment

The impact assessment focuses on evaluating the environmental impacts relevant to each process under study. The climate impact was assessed using the Global Warming Potential (GWP100) indicator in units of kg CO_2-equivalent, based on characterization factors from the IPCC 2021 (Sixth Assessment Report, AR6).

3.4.6 Software and tools for environmental assessment

The environmental impact assessments for both processes were conducted using the Activity Browser (version 2.9.0) [79],For data processing and supporting calculations, Microsoft Excel was utilized due to its flexibility in handling large datasets and performing preliminary analyses. MATLAB [80] was employed to generate plots and visualizations. Process flow diagrams were created using draw.io (also known as diagrams.net), a free online diagramming tool that supports the creation of various flowcharts and process diagrams.

3.5 Economic assessment

In this research, a techno-economic analysis (TEA) will be conducted of two distinct process designs. The objective of this analysis is to evaluate key performance indicators (KPIs): the payback time, the Net Present Value (NPV), and Levelized cost (LC) for each process configuration. This evaluation will provide insights into the economic viability and financial performance of the proposed process designs, enabling a comparison of their cost-effectiveness and profitability.

3.5.1 Cost estimation approach

In this study, Capex includes the direct costs associated with process machinery and equipment, which were derived from vendor quotations and scaled to the target capacity (see Eq. (3.11)). In addition, a process contingency of 15% was applied to account for technical and process-related uncertainties, and an indirect cost factor of 14% was included to cover expenses such as engineering, project management, and site preparation. Costs related to infrastructure, land, installation, and other expenditures were explicitly excluded from the analysis to maintain a focused assessment of the core process technology costs.

$$\mathrm{Capex_i} = \mathrm{Capex_{ref}} \times \left(\frac{\mathrm{C_i}}{\mathrm{C_{ref}}}\right)^{0.6} \tag{3.11}$$

Where:

- $\mathrm{Capex_i}$ and $\mathrm{C_i}$ refer to the equipment cost and capacity of the plant i.
- $\mathrm{Capex_{ref}}$ and $\mathrm{C_{ref}}$ refer to the equipment cost and capacity of the reference plant.

Opex includes three components: (1) Maintenance (4% of Capex annually), (2) Energy costs (electricity at 120 EUR/MWh and cooling water at 0.25 EUR/m^3, both scaling line-

arly with capacity), and (3) Personnel costs. The base personnel requirement was determined according to the reference machinery configuration, then scaled for different capacities using Eg. (3.12).

$$\text{Personnel Cost}_i = \text{Personnel Cost}_{ref} \times \left(\frac{C_i}{C_{ref}}\right)^{0.5} \quad (3.12)$$

Where:

- C_i and C_{ref} refer to capacity i and reference plant

3.5.2 Income estimation

The income potential of the processes is based on two components: (1) Carbon emission permits, where capturing CO_2 leads to cost savings by reducing the need to purchase emission allowances or potential revenue from selling excess credits. An average price of 65 EUR/ton CO_2. (2) Value-added material, specifically precipitated calcium carbonate ($CaCO_3$), produced through the reaction between calcium oxide (CaO) in the feedstock and captured CO_2. The reaction is represented as:

$CaO\ (s)+CO_2(g)\rightarrow CaCO_3(s)$

Based on the CaO content in the feedstock and the molar masses of CaO (56.08 g/mol) and produced $CaCO_3$ (100.09 g/mol), which is governed by conversion efficiency and uptake potential for each process design, the theoretical yield of $CaCO_3$ was calculated and its value estimated using a representative market price of up to 50 EUR/ ton $CaCO_3$. This valuation reflects the unseparated and unpurified state of $CaCO_3$ within the composite matrix, acknowledging that it does not meet the purity standards required for commercial-grade precipitated calcium carbonate.

Table 3.15 summarizes the estimated costs and key parameters for the financial evaluation, based on the thermodynamic analysis and market research for cooling water and energy prices in Austria.

Table 3.15: Summary of estimates for financial assessment

Variable	Value	References
Working hours	8000 hours/year	Own estimation
Lifetime	20 years	Own estimation
Personnel (Opex)	60,000 EUR /Operator for 8 hours daily work	Own estimation
Maintenance (Opex)	4% of Capex	Own estimation

Electricity price (Opex)	120 EUR/MWh	[81]
Natural gas (Opex)	38.66 EUR/MWh	[82]
Cooling water (Opex)	0.25 EUR/m^3	Own estimation
Value-added ($CaCO_3$)	Up to 50 EUR/ton	Own estimation
Carbon credit (Revenue)	65 EUR/ton CO_2	[83]
Tax	23%	[84]
Interest rate	5%	[85]
WACC	8%	Own estimation
Process contingency (Capex)	15% of direct cost	[86]
Indirect cost (Capex)	14% of direct cost	[86]
Ball mill (Capex)	75,000 EUR for 10 ton/h duty	[70]
Stirrer (Capex)	60,000 EUR for 15 m^3/h duty	[70]
Pumping (Capex)	2,500 EUR for 15 m^3/h duty	[70]
RPB (Capex)	200,000 EUR for 12 m^3/h duty	[74]
Liquefaction (Capex)	540,000- 633,000 EUR for 360 kg CO_2/ h duty	[86]
Transport (Capex)	210 EUR/1,000 tkm	[87]
Evaporator (Capex)	70,000 EUR for 360 kg CO_2/h duty	[88]
Carbonator (Capex)	40,000-60,000 EUR for 360 kg CO2/h duty	Own estimation

3.5.3 Payback Period

To calculate the payback period, the initial capital investment must first be established. This investment includes all the upfront costs necessary for implementing the process design, such as equipment procurement, indirect costs, process contingency and other capital expenditures. Next, the annual net cash flow is determined by estimating the annual revenue generated from the process and subtracting the annual operating expenses (Opex). Operating expenses encompass ongoing costs such as maintenance, personnel, energy costs and other operational expenditure [89]. The payback time is then calculated by dividing the total initial capital investment by the annual net cash flow.

$$\text{Payback Period} = \frac{\text{Initial Capital Investment}}{\text{Annual Net Cash Flow}} \tag{3.13}$$

This calculation provides the number of months required to recover the initial investment from the net cash inflows. This method allows for a comparison of the financial viability

and investment attractiveness of different process designs by assessing how quickly the investment can be recouped.

3.5.4 Net present value (NPV)

Net Present Value (NPV) is a fundamental concept in investment analysis that calculates the present value of future cash flows to determine the profitability of an investment project. It is widely used in financial decision-making due to its ability to provide a clear indicator of the potential returns on an investment [90]. NPV (see Eq's (3.14), (3.15)) is considered a key criterion for evaluating the feasibility of projects, alongside other metrics such as Payback Period (PP) [91].

NPV = summation of discounted cash flows over the entire project lifetime (3.14)

$$NPV = \sum_{t=0}^{n} \frac{C_t}{(1+D)^t} \quad (3.15)$$

C_t = inflows at t – outflows at t (3.16)

Where:

- C_t: Cash flow at time t
- D: Discount rate (For Austria WACC is equal to 8% Table 3.15)
- n: Number of periods (is equal to 20 for 20 years of lifetime)

For the calculation of C_t, inflows are the net sales of the value-added products ($CaCO_3$), and the cost saving (carbon credit, Table 3.15) outflows are including the Capex spend (for only 1st year), income tax from EBT (which is 23% in Austria (see table 3.15)), OPEX (personnel, energy, maintenance and RCA cost).

For the calculation of tax:

- EBT = Earnings Before Taxes from project (3.17)
- EBT = Income−OPEX−Depreciation (annualized Capex) −Interest (3.18)

3.5.5 Levelized cost (LC)

Levelized cost (LC) evaluates the economic viability of mineral carbonation projects by calculating the average cost per ton of CO_2 sequestered over the project's lifetime. This metric combines:

- Capex: Initial investments (equipment, process contingency and indirect cost).
- Opex: Lifetime operating costs (energy, personnel, maintenance).
- Exclusion of RCA base cost: Recycled Concrete Aggregate (RCA) was excluded

from the baseline LC calculation due to its dominant cost share, which would obscure comparisons between feedstocks (e.g., steel slag vs. olivine).

$$\text{Levelized Cost} = \frac{\text{Capex} + \sum \text{Opex}}{\text{Total } CO_2 \text{ mineralized over life time}} \quad (3.19)$$

3.5.6 Software tools for Economic Assessment

All economic calculations and modeling of the financial viability of different process configurations were performed using Excel. MATLAB was used for plotting and visualizing the results.

3.5.7 Economic Assessment of RCA-Based CO_2 Mineralization (0.1 kg/s CO_2)

To complement the environmental evaluation, an economic assessment was performed for the base case of mineralizing 0.1 kg CO_2 per second using biogenic CO_2 and 2–4 mm recycled concrete aggregate (RCA) under 60 bar pressure. The scenario assumes zero cost for RCA feedstock and a maximum product value of 50 EUR per ton of $CaCO_3$. The calculated economic metrics include the Capex, Opex and potential revenues, offering insights into the financial feasibility of the process under these baseline conditions.

Table 3.16 Economic Metrics for CO_2 Mineralization (0.1 kg/s, 2–4 mm, 60 bar)

Capex (EUR)	Ball mill	150,000
	Carbonator (for 2-4 mm RCA)	60,000
	Evaporator	70,000
	Liquefaction	540,000
	Process contingency	123,000
	Indirect cost	114,800
Opex (EUR)	Maintenance	42,312
	Personnel	180,000
	Electricity	62,371
	Cooling water	9,816
	Natural gas	8,350
	Transport	12,160
Revenue	Value added product ($CaCO_3$) (EUR/year)	310,920
	Carbon credit (EUR/year)	177,840
KPI's	Levelized cost (EUR/ton CO_2)	127.7
	Payback (months)	86
	NPV (EUR/ 20-year lifetime)	1,992,024

3.5.8 Economic assessment of Steel Slag carbonation (100 kg CO_2/hour)

To complement the environmental assessment, a preliminary economic analysis was conducted for the base case scenario of mineralizing 100 kg CO_2 per hour, which corresponds to processing approximately 513 kg of steel slag per hour. This setup represents a continuous operation of 8,000 hours per year. Table 3.17 summarizes Capex, Opex and revenue streams based on two major income categories: carbon credits and the sale of calcium carbonate ($CaCO_3$) as a value-added product.

Table 3.17: Economic Metrics: 100 kg CO_2/h Scenario

Capex (EUR)	Ball mill	12,622
	Stirrer	48,992
	Pump	2,041
	RPB	163,307
	Process contingency	34,044
	Indirect cost	31,775
Opex (EUR)	Maintenance	12,918
	Personnel	60,000
	Electricity	8,160
Revenue	Value added product ($CaCO_3$) (EUR/year)	84,500
	Carbon credit (EUR/year)	48,360
KPI's	Levelized cost (EUR/ton CO_2)	126.59
	Payback (months)	226
	NPV (EUR/ 20-year lifetime)	84,837

This base case serves as a foundation for scaling analysis and techno-economic comparisons of larger facilities.

4 Results and Discussion

4.1 LCA of size fraction effects for base case (0.1kg/s CO_2)

As the first step in evaluating the environmental performance of the mineralization process, a Life Cycle Assessment (LCA) was conducted for the base case of 0.1 kg/s CO_2, consistent with the methodology described earlier. The focus was placed on two critical unit operations whose scale and energy demands vary as a function of the size fraction of the Recycled Concrete Aggregate (RCA).

The LCA calculations were performed under two scenarios. The first scenario assumed a high steel recovery rate of 95%, as described in section 3.4.4 using the MaTrace Global model, which accounts for material recovery and recycling flows at end of life. The second scenario represented a worst-case assumption of no steel recovery. As expected, the environmental contribution from equipment construction reaches its maximum under the no-recovery scenario. The amount of steel required increases with the RCA particle size, because larger fractions exhibit lower CO_2 uptake per ton. Consequently, more RCA must be processed to mineralize the same amount of CO_2, which requires additional crushing and reaction capacity. Interestingly, despite the increase in total RCA mass at larger size fractions, the overall energy consumption of the crushing process decreases. This is due to the lower specific energy requirement (expressed in kWh per ton RCA) at larger particle sizes, following the Bond equation (see Eq.3.8), which describes the energy needed to reduce material size from 10 mm to finer fractions (see Table 3.8).

As a result, even though larger RCA fractions demand higher construction requirements, they remain environmentally more favourable across the seven size fractions considered.

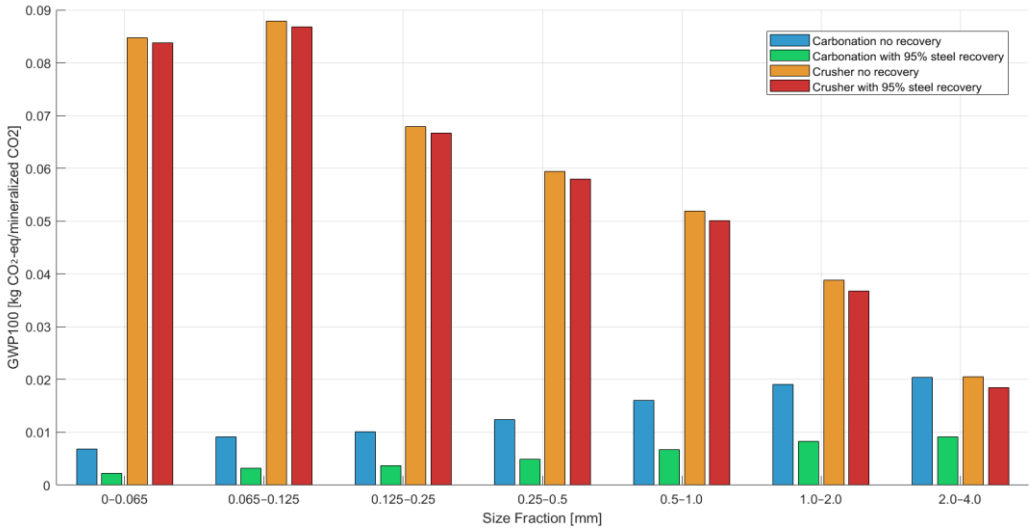

Fig. 4.1 GWP by size fraction and steel recovery

Table A.2 (Appendix) presents the Life Cycle Inventory (LCI) used for the calculation of the climate change impact (GWP) under the two steel recovery scenarios and across seven particle size fractions. The results shown in Fig. 4.1 are based on this LCI and include contributions from both processes. While Fig. 4.2 shows the detailed LCA results for the base case (0.1kg/s) with 95% steel recovery, with a breakdown of energy use and construction impacts to illustrate the trends across size fractions.

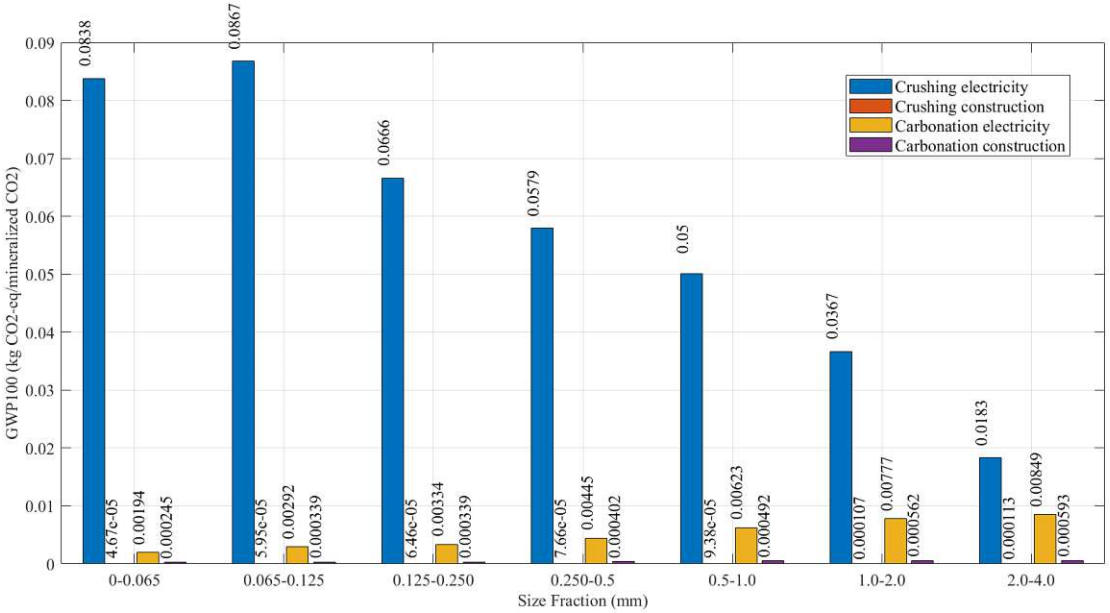

Fig. 4.2 GWP contributions by size fraction and unit operation

The data clearly shows that the contribution of electricity consumption is significantly higher than that of construction across all size fractions. However, from a financial perspective, this environmentally favorable outcome is not necessarily feasible. Even when assigning a value of 50 EUR per ton to the precipitated calcium carbonate ($CaCO_3$) produced, utilizing larger recycled concrete aggregate (RCA) particle sizes for CO_2 mineralization remains financially unfeasible. This is due to the increased quantity of RCA required to achieve equivalent CO_2 uptake, coupled with RCA costs ranging up to 12 EUR per ton in Europe [92].

4.2 LCA of CO_2 Delivery Pressure Effects for Base Case (0.1 kg/s CO_2)

As an additional step in evaluating the environmental performance of the mineralization process, an LCA was conducted to assess the impact of varying CO_2 delivery pressures under the base case of 0.1 kg/s CO_2. This scenario addresses how the conditions of liquefied CO_2, particularly the delivery pressure, influence the LCI. The analysis focused on two critical unit operations, liquefaction and evaporation, whose energy demands are affected

by CO_2 pressure. Changes in delivery pressure affect not only the compression work and cooling duty required in the liquefier but also the thermal energy demand in the evaporator. Consequently, the changes in LCI ultimately influence the Global Warming Potential (GWP) associated with each delivery pressure scenario, allowing for a more comprehensive assessment of the environmental trade-offs.

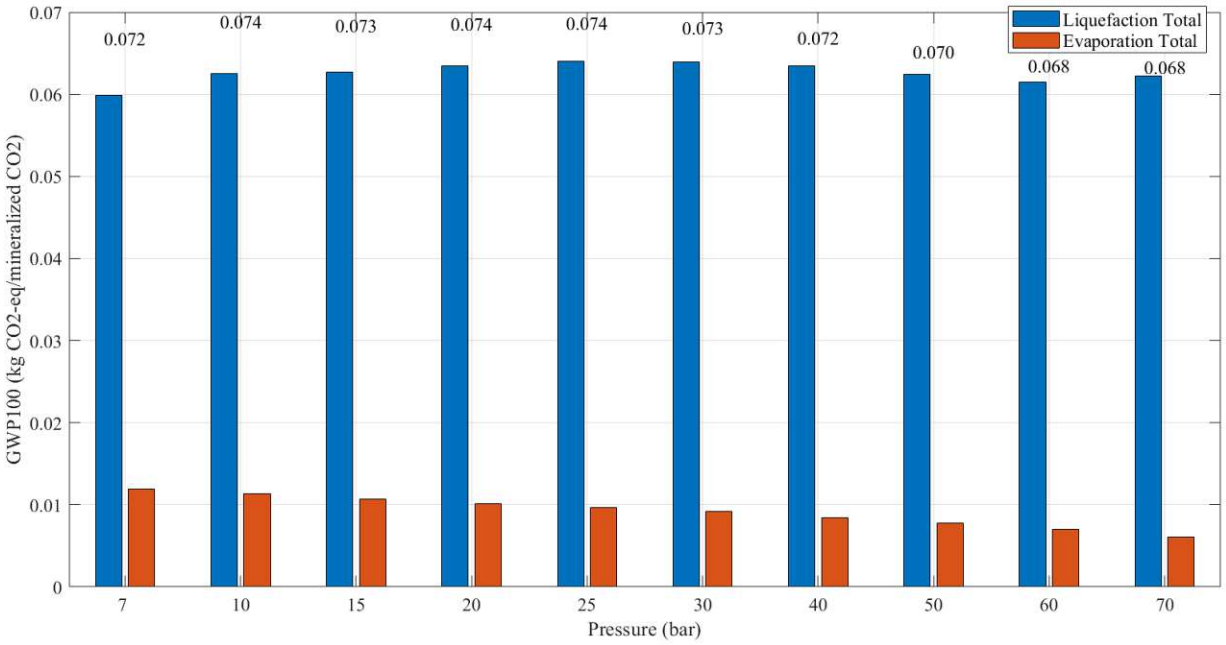

Fig. 4.3: GWP of CO_2 delivery pressure for Liquefaction and Evaporation (0.1 kg/s CO_2)

Figure 4.3 shows the GWP for liquefaction and evaporation at varying CO_2 delivery pressures under the base case of 0.1 kg/s CO_2. While GWP increases with pressure, the total GWP is lowest at 60 bar, indicating that this pressure offers the optimal balance between energy demand and environmental impact. The GWP values at 60 bar are notably lower than at other pressures, suggesting that 60 bar is the most environmentally sustainable choice for CO_2 delivery in the mineralization process. Table A.3 (Appendix) presents the Life Cycle Inventory (LCI) used for calculating the climate change impact (GWP100) under the high steel recovery scenario (95%). The LCI includes the Technosphere flows for the liquefaction and evaporation unit operations, which form the basis for the results shown in Fig. 4.3.

To better understand the sources of climate change impact, the contribution of individual energy segments within the liquefaction and evaporation unit operations was analyzed. For evaporation, the heating duty was evaluated, while for liquefaction, the NH_3 refrigeration cycle, intercooling system, and compression train were considered. Since the construction

material (assumed mainly as steel and considered 95% recovered after its lifetime) has a minor impact, only energy-related contributions are shown. Figure 4.4 presents the breakdown of energy-related Global Warming Potential (GWP100) for two-unit operations: liquefaction (including the compression train, intercooling system, liquefier, and NH_3 cycle system) and evaporation.

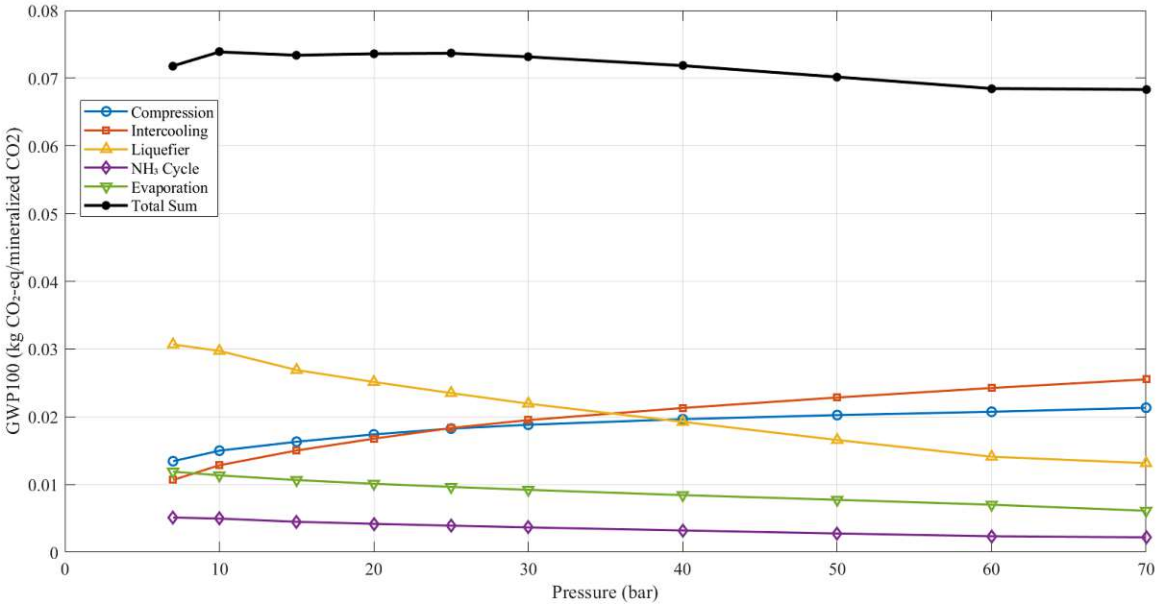

Fig. 4.4 GWP of Liquefaction and Evaporation by pressure

As pressure increases, the energy demand and associated climate impact from liquefaction components initially fluctuate but reach the lowest point at 60 bar. While the evaporation heating duty slightly decreases with pressure, its contribution remains smaller compared to liquefaction. From an environmental perspective, operating at 60 bar is the best choice, as it minimizes the total energy requirement and associated climate impact. The next step of the assessment will broaden to calculate the LCA of all process steps, including liquefaction, storage and transport, evaporation, carbonation, and grinding (see Fig. 4.5). For consistency with the previous findings, the CO_2 delivery pressure will be set at 60 bar, and the results will be presented across different RCA size fractions. The focus so far has been mainly on energy-related impacts, as the calculations showed that the share of energy is much higher than that of construction materials. Moreover, since changes in the capacity of different biogas plants do not affect energy consumption per functional unit, these findings are expected to be valid across all biogas production scales.

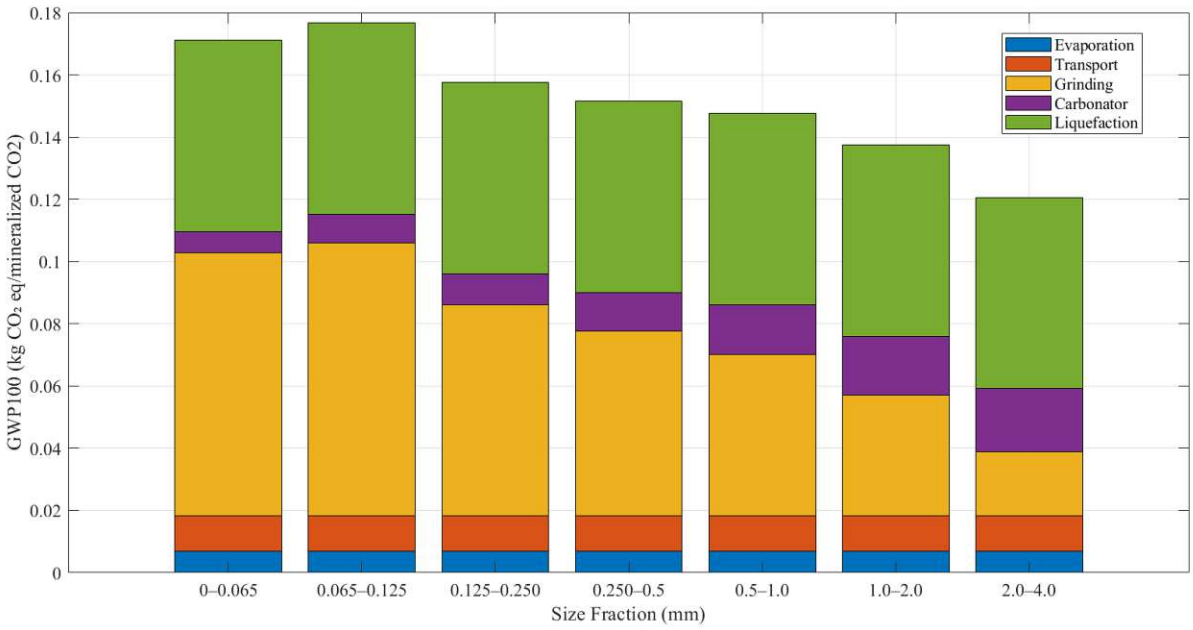

Fig. 4.5 GWP100 by RCA Size Fraction at 60 bar CO_2 delivery pressure

Fig. 4.5 illustrates the total environmental impact of the process model for mineralizing biogenic CO_2 (a byproduct of biogas plant) at the optimal delivery pressure of 60 bar and for 0.1 kg/s CO_2, identified as the most favourable from an environmental perspective. While the impact contributions of liquefaction, evaporation, and transport remain constant across RCA size fractions, the contributions from crushing and the carbonator vary with the size fraction. This approach was taken because, although coarser size fractions are environmentally preferable, they may not be financially feasible at all RCA pricing levels (see Section 4.3, Financial Assessment). Therefore, a trade-off between environmental and financial performance needs to be considered.

4.3 Economic Assessment for mineralization of biogenic CO_2

In this section, the results of the techno-economic analysis (TEA) process designs are presented. The evaluation focuses on the key performance indicators (KPIs) identified in Section 3.5, namely: the payback period, Net Present Value (NPV), and Levelized Cost (LC). Each of these metrics is discussed in terms of their significance for assessing the economic viability of the process designs.

4.3.1 Levelized cost

As a base case, a levelized cost of 127.7 EUR/ton CO_2 was calculated for a system designed

to process 0.1 kg/s of CO_2. For the biogas plants in Austria, the levelized costs were assessed based on the mineralization efficiency of 0.95% presented in Table 4.1.

Table 4.1 Levelized Cost Analysis for Austrian Biogas Plants

	Bruck a.d.Leitha	EVN	Engerwitzdorf	Häusle	Reitbach	Steindorf	Zemka	Pfaffenau	Wiener Neustadt Süd	Steiermark	11 er Nahrungsmittel GmbH
Annualized Capex (EUR/ton CO_2)											
Ball mill	2.46	2.08	4.04	2.61	3.30	3.44	3.54	3.96	3.82	4.35	2.39
Liquefaction	9.88	8.39	16.3	10.5	13.3	13.8	14.2	15.9	15.4	17.5	9.65
Evaporation	1.13	0.96	1.85	1.19	1.51	1.57	1.62	1.82	1.75	2	1.1
Carbonation	0.97	0.82	1.59	1.03	1.3	1.35	1.4	1.56	1.50	1.71	0.94
Process contingency	2.16	1.84	3.56	2.30	2.90	3.03	3.12	3.49	3.37	3.84	2.11
Indirect cost	2.02	1.72	3.32	2.15	2.72	2.83	2.91	3.26	3.14	3.58	1.92
Opex (EUR/ ton CO_2)											
Maintenance	14.9	12.65	24.5	15.83	20	20.8	21.4	24	23.16	26.41	14.53
Personnel	52.6	39.55	125	58.55	88.3	94.9	99.5	121.3	113.9	143.4	50.4
Electricity	22.8	22.8	22.8	22.8	22.8	22.8	22.8	22.8	22.8	22.8	22.8
Natural Gas	3.05	3.05	3.05	3.05	3.05	3.05	3.05	3.05	3.05	3.05	3.05
Cooling Water	3.6	3.6	3.6	3.6	3.6	3.6	3.6	3.6	3.6	3.6	3.6
Transport	4.4	4.4	4.4	4.4	4.4	4.4	4.4	4.4	4.4	4.4	4.4
Levelized cost	120	101.8	214	128	167	175.6	181	209.1	199.8	236.6	116.8

The analysis reveals that plants with higher CO_2 processing capacities generally achieve lower levelized costs, illustrating the benefit of economies of scale. For example, EVN (5,959 ton/year), 11er Nahrungsmittel GmbH (4,210 ton/year), and Bruck a.d. Leitha (3,960 ton/year) show relatively lower levelized costs due to the distribution of capital and

operational expenses over larger CO_2 volumes. In contrast, smaller plants such as Steiermark (946 ton/year), Zemka (1,141 t/year), and Reitbach (1,201 ton/year) exhibit significantly higher levelized costs. This variation underscores the influence of plant capacity on cost efficiency, where Capex and operational cost such as maintenance and personnel are more effectively allocated in larger-scale operations.

4.3.2 Payback Period

The payback period indicates how quickly the investment can be recovered for each process design. In contrast to the environmental assessment, where RCA did not carry any environmental burden, the RCA price as part of the operational costs has the strongest influence on the economic feasibility of the process design. As shown in Section 4.2, the coarser RCA size fractions deliver the most favorable environmental performance. However, if the RCA price is assumed at 12 EUR per ton, the process is unable to recover its initial investment solely through the combined revenues from carbon credits (65 EUR per ton CO_2) and the value-added potential of the carbonated RCA with embedded $CaCO_3$. Furthermore, the value-added product itself presents an economic limitation: in the current process design, no additional steps are included to separate or purify the $CaCO_3$ as a target product. While the market price for pure $CaCO_3$ in Europe is approximately 210 EUR per ton [93], a realistic assumption for the mixed carbonated RCA product may be no more than 50 EUR per ton. If the price of RCA is set to zero, reflecting a scenario where it undergoes carbonation primarily to improve its mechanical properties (such as 28-day compressive strength) before being partially substituted for construction materials [54], and the $CaCO_3$(embedded in the matrix of the carbonated RCA) is valued at 30 EUR per ton, the process would be able to recover its initial investment after approximately 215 months. Under these conditions, the project would achieve a Net Present Value (NPV) of over 250,000 EUR at the end of its 20-year lifetime. Figure 4.6 illustrates how variations of product value influence the overall economic feasibility of the process. This analysis is based on the base case scenario, which assumes a CO_2 flow rate of 0.1 kg/s in the mineralization process, as used in the different designs and calculations throughout this study. The figure highlights the sensitivity of the cost recovery to these key parameters, emphasizing the uncertainty associated with the value added from the carbonated product.

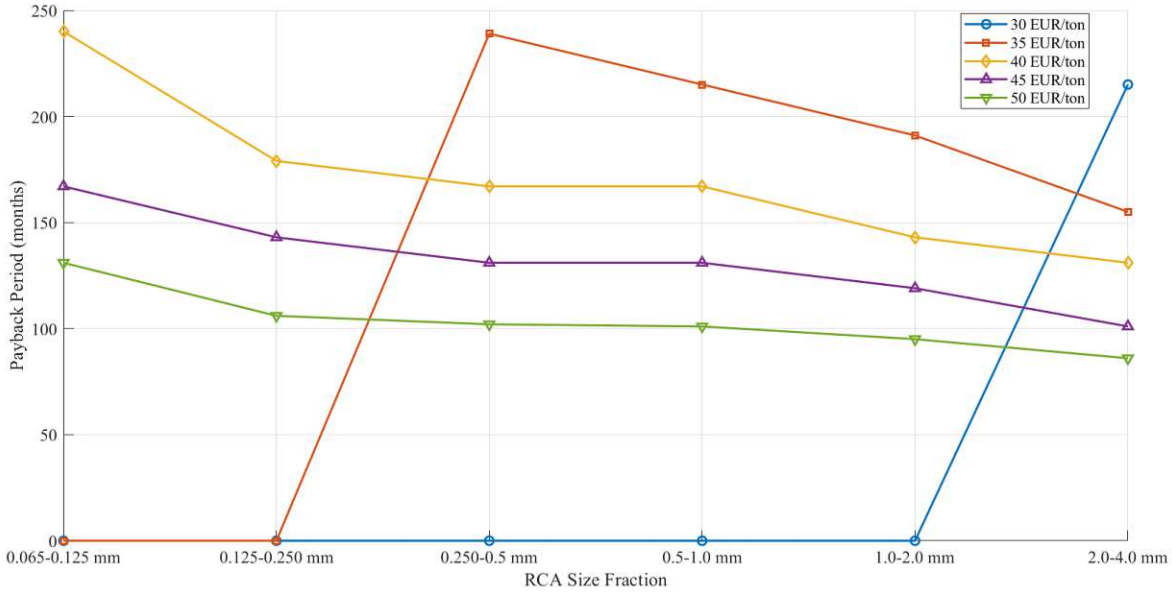

Fig. 4.6 Effect of RCA size and product value on Process Payback Time

The results show that larger RCA size fractions assessed in this study are associated with shorter payback periods (in months), enabling faster recovery of the initial investment. Although the total quantity of RCA changes between size fractions, it was considered a cost-free input in the base case scenario. Therefore, the main cost difference across sizes comes from the energy required for crushing and size reduction. Furthermore, the analysis indicates that under the current process design, even a modest RCA price above 1EUR per ton results in unfeasible project economics, as the process can no longer recover its initial investment within the assumed 20-year lifetime. At this price level, only the smallest size fraction (0–0.065 mm), which requires the least amount of RCA to mineralize a given CO_2 flow rate (0.1 kg/s), remains economically feasible.

In an alternative scenario, both the RCA price and the value-added product are assumed to be zero, meaning the process is undertaken solely to improve the mechanical properties of the RCA. Despite this simplified revenue structure, the project's feasibility remains challenged by significant operational costs (notably energy and personnel costs).

For this sensitivity analysis it is assumed:

- Electricity price: Varying (80–130 EUR/MWh)
- Personnel Costs: Only indirect costs (project management and engineering, assumed to be 14% of the direct costs, including equipment) are considered
- Other Costs: remain unchanged from the base case

The table below summarizes the resulting payback periods (in months) for seven distinct RCA size fractions as the electricity cost is varied. (Note: cells showing "N/A" indicate

cases where the process is not economically feasible, as they cannot cover the investment cost during the lifetime of the plant.

Table 4.2 Effect of electricity price on RCA carbonation payback (months)

Electricity price (EUR/MWh)	RCA particle size (mm)						
	0-0.065	0.065-0.125	0.125-0.250	0.250-0.50	0.50-1.0	1.0-2.0	2.0-4.0
80	NA	NA	NA	239	239	215	191
85	NA	NA	NA	NA	NA	227	191
90	NA	NA	NA	NA	NA	227	191
95	NA	NA	NA	MA	NA	239	203
100	NA	NA	NA	NA	NA	NA	203
105	NA	NA	NA	NA	NA	NA	215
110	NA	NA	NA	NA	NA	NA	215
115	NA	NA	NA	NA	NA	NA	227
120	NA	NA	NA	NA	NA	NA	227
130	NA	NA	NA	NA	NA	NA	239

While RCA price and product value are key economic drivers, this analysis shows that even without considering them, high electricity and personnel costs significantly impact feasibility. As the main contributors to operational expenses, these factors highlight the strong dependence of process viability on energy pricing, staffing strategy, and resource availability.

4.3.3 Payback Time and Plant-Specific Results

Figure 4.5 highlights how larger-scale plants benefit from favorable cost dynamics, leading to shorter payback times and more attractive NPVs. Economies of scale are evident: capital expenditure components were scaled using a 0.6 exponent, as detailed in the methodology, and personnel costs were assumed to be scaled using a 0.5 exponent with plant size. For example, EVN, with an annual CO_2 capacity roughly three times higher than Reitbach, incurs a personnel cost of only 223,878 EUR per year compared to 158,633 EUR for Reitbach. This disproportionate growth in cost versus capacity results in significantly improved

economic performance for larger plants. Thus, scale not only enhances CO_2 abatement potential but also improves investment feasibility.

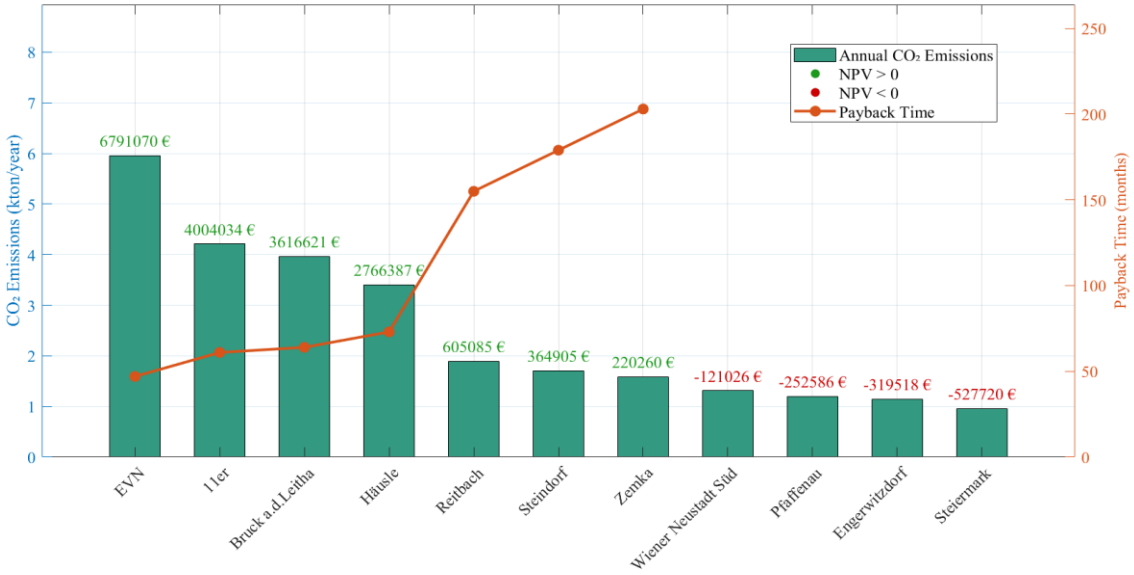

Fig. 4.7 Economics vs Scale in CO_2 Mineralization

4.4 LCA for base case Steel Slag Carbonation

Table 4.2 presents the life cycle inventory data used for modeling the base case scenario in the environmental assessment. Technosphere flows represent material and energy inputs per functional unit of 1 kg of CO_2 mineralized. A carbonation efficiency of 96% is applied, as reported by [41]. The system boundary includes material supply, energy use in processing units, and infrastructure requirements (e.g., RPB, crusher). 95% steel recovery is assumed as the output flows. the steel slag is treated as a burden-free by-product at the system boundary. No upstream environmental impacts are assigned to the slag itself, as it is derived from existing steel production processes and would otherwise be considered waste.

Table 4.3 Life Cycle Inventory for Base Case (100kg/h CO_2)

Technosphere flows	Location	Unit	Unit Operations			
			Ball Mill	Stirrer	Pumping	RPB
Electricity, medium voltage	AT	kWh	0.05094	0.01083	0.004479	0.02229
Steel, chromium steel 18/8	RER	kg	1.4974E-05	1.1E-05	4.883E-07	2.389E-06
Metal working, average for chromium steel product manufacturing	RER	kg	1.4974E-05	1.1E-05	4.883E-07	2.389E-06

LCA results showing the GWP (kg CO_2-eq), for each unit operation, divided into operational (electricity) and construction-related (steel) contributions.

Table 4.4 GWP by Unit Operation: Operational vs. Construction Contributions

Contributions	GWP (kg CO_2 eq. / kg CO_2 mineralized)			
	Ball Mill	Stirrer	Pumping	RPB
Operational-related (electricity)	0.013188	0.002804	0.00116	0.005771
Construction-related (steel)	0.000104	7.6E-05	3.39E-05	1.66E-05

As shown in Table 4.3, the electricity used across the various unit operations contributes the highest share to GWP. Given the significant impact of electricity consumption, a sensitivity analysis will be conducted, comparing the current electricity (medium voltage in Austria) with alternative energy sources. This analysis aims to evaluate how different eletricity production scenarios might influence the overall environmental performance of the process.

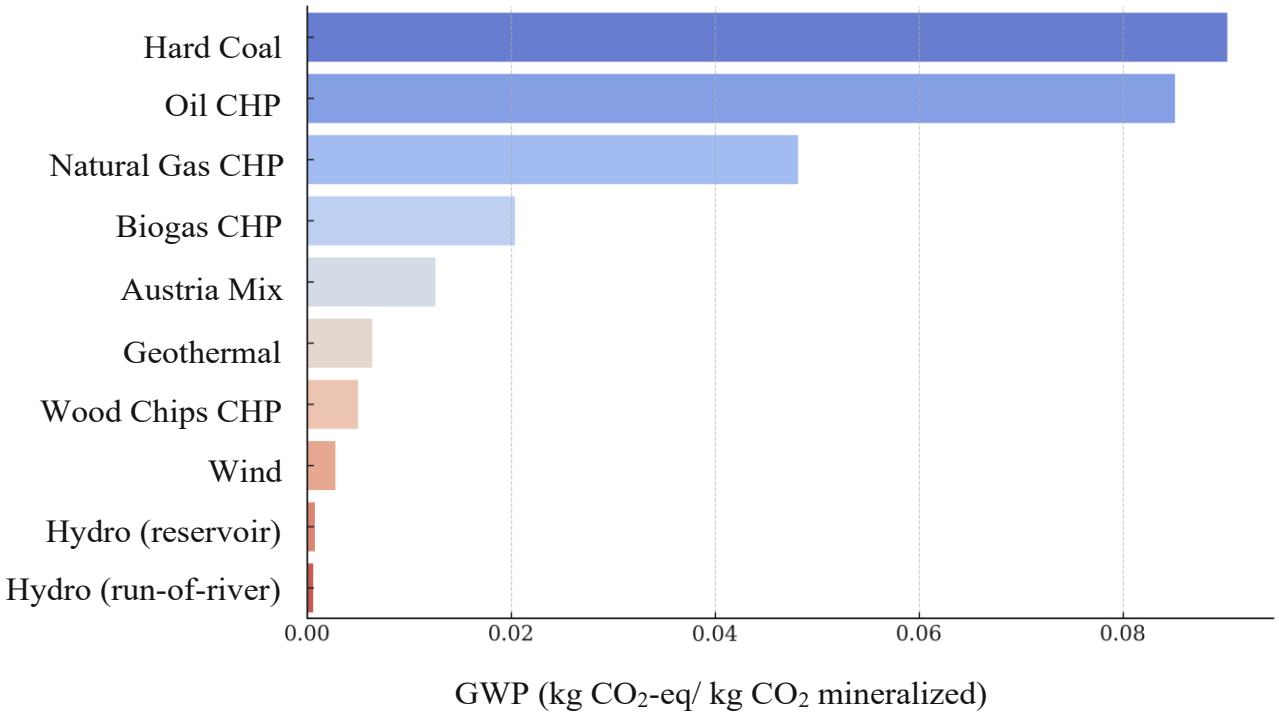

Fig. 4.8: GWP of steel slag carbonation under different electricity sources in Austria

The maximum GWP value was observed for the "Heat and power co-generation, hard coal" scenario, reaching 0.0902 kg CO_2-eq per kg CO_2 mineralized, while the minimum value was recorded for the "Electricity, hydro, run-of-river" scenario at 0.00057 kg CO_2-eq per kg CO_2 mineralized. On the other hand, as previously demonstrated, the contribution of electricity-related emissions dominates the GWP, whereas the scale of the different Austrian steelmaking plants does not influence the GWP per unit operation. Consequently, these values are applicable across all evaluated plant configurations and are valid for the assumptions and process design considered in this study. For the five Austrian steelmaking plants considered in this study, and under the assumption of 96% CO_2 mineralization efficiency, the Table 4.4 presents the CO_2 captured capacity in terms of GWP per kg CO_2 mineralized for different electricity sources. These values reflect the environmental impact per unit of CO_2 captured and highlight the significant influence of the electricity mix used in the process.

Table 4.5 Theoretical CO_2 Capture Potential by Electricity Source

Electricity sources	Total theoretical CO_2 capture potential (ton)				
	Edelstahl Mitterdorf	Voestalpine Donawitz	Voestalpine Linz	Edelstahl Kapfenberg	Stahlwerk Marienhütte
Hard coal	2,414.87	137,015.25	436,973.49	14,601.01	4,308.34
Oil, CHP	2,428.49	137,788.31	439,438.96	14,683.39	4,332.65
Natural gas, CHP	2,526.57	143,353.01	457,186.09	15,276.39	4,507.62
Austria mix	2,621.01	148,711.14	474,274.41	15,847.38	4,676.11
Biogas, CHP	2,600.34	147,538.37	470,534.19	15,722.40	4,639.23
Geothermal	2,637.43	149,642.79	477,245.65	15,946.66	4,705.40
Wood chips, CHP	2,637.43	149,854.84	477,921.94	15,969.26	4,712.07
Wind	2,647.02	150,492.02	478,982.10	16,004.68	4,722.52
Hydro (reservoir)	2,652.40	150,492.02	479,954.06	16,037.16	4,732.10
Hydro (run of river)	2,652.88	150,519.54	480,041.82	16,040.09	4,732.97

4.5 Economic Assessment for Slag carbonation

4.5.1 Levelized cost

This metric represents the cost of capturing and mineralizing one ton of CO_2, integrating both capital and operational expenditures over the system's lifetime. It provides a standardized basis for economic comparison between the plants, dependent on their size or throughput.

Table 4.6: Summary of Levelized Cost per Ton CO_2 Captured

	Edelstahl Mitterdorf	Voestalpine Donawitz	Voestalpine Linz	Edelstahl Kapfenberg	Stahlwerk Marienhütte
Annualized Capex (EUR/ton CO_2)					
Ball mill	0.50	0.1	0.06	0.24	0.40
Stirrer	1.94	0.39	0.24	0.95	1.54
Pump	0.08	0.02	0.01	0.04	0.06
RPB	6.47	1.29	0.81	3.15	5.14

Process contingency	1.35	0.27	0.17	0.66	1.07
Indirect cost	1.26	0.25	0.16	0.61	1.00
Opex (EUR/ ton CO_2)					
Maintenance	7.20	1.43	0.90	3.50	5.71
Personnel	42.02	5.58	3.12	17.09	31.46
Electricity	10.63	10.63	10.63	10.63	10.63
Levelized cost	71.45	19.94	16.10	36.87	57.01

The levelized cost of CO_2 mineralization expressed in EUR per ton of CO_2 captured, varies significantly across the evaluated steel plants and is strongly influenced by plant size. As the data indicate, larger facilities such as Voestalpine Stahl Linz and Voestalpine Stahl Donawitz GmbH benefit from economies of scale, achieving notably lower LC values of 16.10 and 19.94 (EUR/ton CO_2), respectively. In contrast, smaller plants like Edelstahl Mitterdorf and Stahlwerk Marienhütte GmbH show considerably higher LC values, reaching 71.45 and 57,01 (EUR/ton CO_2). This is primarily due to the disproportionate impact of fixed costs, particularly capital investment in the Rotating Packed Bed (RPB) units and high personnel costs that do not scale linearly with processing capacity. Among the operational costs, electricity is constant across all cases (10.63 EUR/ton CO_2), suggesting standardized energy use per ton captured. Overall, these results emphasize the critical role of scale in reducing the cost of mineralization and highlight the importance of capacity optimization for achieving economic viability in industrial CO_2 removal through steel slag carbonation.

4.5.2 Economic Feasibility Assessment: NPV and Payback Period Analysis

Following the presentation of the Levelized Cost (LC), which primarily reflects the cost-efficiency of CO_2 mineralization, this section shifts focus to the economic feasibility of the process by introducing two key financial indicators: Net Present Value (NPV) and Payback Period. Unlike LC, which does not account for revenue streams, NPV and Payback Period incorporate both costs and projected income, offering a more comprehensive evaluation of financial viability. These metrics are calculated based on the assumptions detailed in Table 3.15, including discount rate, project lifetime, and WACC also expected revenues from

carbon credits and the sale of calcium carbonate as a value-added product (up to 50 EUR/ton $CaCO_3$) which were presented in Table 4.6.

Table 4.7 Economic Feasibility of CO_2 Mineralization by Plants

	Edelstahl Mitterdorf	Voestalpine Donawitz	Voestalpine Linz	Edelstahl Kapfenberg	Stahlwerk Marienhütte
Capex (EUR)					
Ball mill	26,564.08	299,654	600,941	78,197	37,596
Stirrer	103,107.40	1,163,094	2,332,527	303,517	145,928
Pump	4,296.14	48,462	97,189	12,647	6,080
RPB	343,691.35	3,876,981	7,775,090	1,011,724	486,428
Process contingency	71,648.85	808,229	1,620,862	210,913	101,405
Indirect cost	66,872.26	754,347	1,512,805	196,852	94,645
Opex (EUR)					
Maintenance	19,106.36	215,528	432,230	56,243	27,041
Personnel	111,545.95	840,217	1,500,495	274,283	148,992
Electricity	28,207.96	1,600,468	5,104,263	170,554	50,325
Revenue (Million EUR)					
Carbon Credit	0.167	9.483	30.245	1.011	0.298
Value added material ($CaCO_3$)	0.3	16.6	52.8	1.8	0.5
KPI's (NPV and Payback Period) (for Value added = 50 EUR/ton)					
Payback time (months)	37	4	2	12	24
NPV (Million EUR)	2.78	312.48	1,032.3	27.94	6.34

Because the market value of calcium carbonate ($CaCO_3$) as a by-product significantly influences the overall economic performance, it is treated as a critical parameter in assessing the financial viability of this process. To better understand its impact, a sensitivity analysis was performed considering six different pricing scenarios for $CaCO_3$, ranging from low to high market values. This analysis aims to capture the variability in potential revenues and its effect on Payback Period across all evaluated plants. The outcomes of this analysis are

visualized in Table 4.7, providing a comparative view of how each plant's financial performance shifts under different value assumptions.

Table 4.8 Sensitivity to By-Product Value: Payback Periods for Evaluated Plants

Price (EUR/ton$CaCO_3$)	Edelstahl Mitterdorf	Voestalpine Donawitz	Voestalpine Linz	Edelstahl Kapfenberg	Stahlwerk Marienhütte
	Payback period (months)				
0	NA	15	8	76	NA
10	NA	10	6	36	161
20	172	7	4	24	66
30	77	6	3	17	41
40	50	5	3	14	30
50	37	4	2	12	24

5 Conclusion

This study investigated the enviromental and economic feasibility of carbon mineralization in Austria through two distinct pathways: (1) biogenic CO_2 utilization via carbonation of recycled concrete aggregates (RCA) and (2) industrial CO_2 utilization through steel slag carbonation. The results demonstrate that both routes are environmentally viable, though their economic performance varies significantly depending on site-specific conditions and market factors.

In the case of RCA carbonation, environmental performance was most favourable at coarser particle sizes (2–4 mm), achieving a Global Warming Potential (GWP) of 0.12 kg CO_2-eq per kg of CO_2 sequestered (at 60 bar). This is attributed to the lower energy demand for crushing larger particles. However, the economic assessment revealed that this pathway is currently not viable under prevailing market conditions, With RCA priced above 1 EUR/ton and $CaCO_3$ valued below 50 EUR/ton. The levelized costs range from 127.7 EUR/ton CO_2 at optimal conditions (60 bar pressure, zero RCA cost and for 0.1 kg/s CO_2). Although these figures suggest economic infeasibility, the scenario could become more attractive if RCA were sourced at no cost and if the process were powered by low-carbon electricity, such as hydropower.

From an environmental perspective, steel slag carbonation achieved a low global warming potential (GWP) of 0.023 kg CO_2-eq per kg of CO_2 mineralized. While this value is lower on a per-unit basis compared to the biogenic CO_2 route, it must be noted that biogenic CO_2 is carbon-neutral at the source.

From an economic standpoint, the base-case scenario, assuming a CO_2 flow rate of 100 kg/h, resulted in levelized costs of 126.59 EUR per ton of CO_2 mineralized. However, significant cost reductions were observed at larger scales. For instance, in an industrial setting such as Voestalpine Linz, the levelized cost dropped to 16.10 EUR/ton, highlighting the impact of economies of scale. Furthermore, unlike the RCA-based process, the steel slag carbonation setup benefits from on-site availability of both CO_2 and mineral feedstock, eliminating the need for energy-intensive unit operations such as CO_2 liquefaction and evaporation, as well as transportation. These factors contribute to reduced capital and operational expenditures. The reported costs strictly represent the average cost of CO_2 mineralization over the project lifetime and exclude potential revenues from carbon credits or the valorisation of by-products.

Despite these positive indicators, both pathways face significant challenges. High energy

costs, the pricing of RCA, and the low market value of carbonated by-products present major barriers to commercialization.

To advance the deployment of carbon mineralization technologies in Austria, future efforts should focus on several strategic areas. First, pilot-scale validation is needed for both RCA and steel slag carbonation processes to confirm technical assumptions and refine operational efficiencies. The integration of on-site renewable energy sources, such as solar or wind, could further reduce the carbon footprint and improve cost-effectiveness.

From an economic perspective, developing higher-value applications for carbonated RCA, particularly in the construction sector, would help diversify revenue streams and enhance financial viability. Additionally, advocacy for carbon credit mechanisms and targeted tax incentives is crucial to offset high capital and operating costs, especially during the early stages of commercialization.

System expansion strategies should also be explored. These include hybrid systems that combine biogenic and industrial CO_2 sources to maximize overall sequestration potential, as well as fostering industrial symbiosis. For example, between cement and steel producers, to create circular supply chains that reuse RCA and slag by-products.

In the long term, with sufficient policy support and continued technological development, carbon mineralization could make a meaningful contribution to Austria's 2040 climate neutrality targets, particularly in hard-to-abate sectors like construction and steel production. The findings of this study may support future research, pilot initiatives, and planning efforts aimed at advancing carbon mineralization from the lab to industrial application.

List of References

[1] publikationsdetail n.d. https://www.umweltbundesamt.at/studien-reports/publikationsdetail (accessed June 21, 2025).

[2] Tol RSJ. The Economic Effects of Climate Change. J Econ Perspect 2009;23:29–51. https://doi.org/10.1257/jep.23.2.29.

[3] Uğurlu E. Renewale Energy Sources and Climate Change Mitigation. In: Kurochkin D, Crawford MJ, Shabliy EV, editors. Energy Policy Adv. Clim. Change Mitig. Int. Environ. Justice, Cham: Springer International Publishing; 2022, p. 69–92. https://doi.org/10.1007/978-3-030-84993-1_4.

[4] Rogelj J, Popp A, Calvin KV, et al. Scenarios towards limiting global mean temperature increase below 1.5 °C. Nat Clim Change 2018;8:325–32. https://doi.org/10.1038/s41558-018-0091-3.

[5] Muratori M, Bauer N, Rose SK, et al. EMF-33 insights on bioenergy with carbon capture and storage (BECCS). Clim Change 2020;163:1621–37. https://doi.org/10.1007/s10584-020-02784-5.

[6] Rosa L, Sanchez DL, Mazzotti M. Assessment of carbon dioxide removal potential via BECCS in a carbon-neutral Europe. Energy Environ Sci 2021;14:3086–97. https://doi.org/10.1039/D1EE00642H.

[7] Geden O, Peters ,Glen P., and Scott V. Targeting carbon dioxide removal in the European Union. Clim Policy 2019;19:487–94. https://doi.org/10.1080/14693062.2018.1536600.

[8] Müller LJ, Kätelhön A, Bachmann M, et al. A Guideline for Life Cycle Assessment of Carbon Capture and Utilization. Front Energy Res 2020;8. https://doi.org/10.3389/fenrg.2020.00015.

[9] Thengane SK, Tan RR, Foo DCY, et al. A Pinch-Based Approach for Targeting Carbon Capture, Utilization, and Storage Systems. Ind Eng Chem Res 2019;58:3188–98. https://doi.org/10.1021/acs.iecr.8b06156.

[10] Ho H-J, Iizuka A, Shibata E. Carbon Capture and Utilization Technology without Carbon Dioxide Purification and Pressurization: A Review on Its Necessity and Available Technologies. Ind Eng Chem Res 2019;58:8941–54. https://doi.org/10.1021/acs.iecr.9b01213.

[11] Bruhn T, Naims H, Olfe-Kräutlein B. Separating the debate on CO2 utilisation from carbon capture and storage. Environ Sci Policy 2016;60:38–43.

https://doi.org/10.1016/j.envsci.2016.03.001.

[12] Talapaneni SN, Singh G, Kim IY, et al. Nanostructured Carbon Nitrides for CO2 Capture and Conversion. Adv Mater 2020;32:1904635. https://doi.org/10.1002/adma.201904635.

[13] Cuéllar-Franca RM, Azapagic A. Carbon capture, storage and utilisation technologies: A critical analysis and comparison of their life cycle environmental impacts. J CO2 Util 2015;9:82–102. https://doi.org/10.1016/j.jcou.2014.12.001.

[14] Al-Mamoori A, Krishnamurthy A, Rownaghi AA, et al. Carbon Capture and Utilization Update. Energy Technol 2017;5:834–49. https://doi.org/10.1002/ente.201600747.

[15] Carceller A, Guillén M, Álvaro G. Lactic Acid from CO2: A Carbon Capture and Utilization Strategy Based on a Biocatalytic Approach. Environ Sci Technol 2023;57:21727–35. https://doi.org/10.1021/acs.est.3c05455.

[16] Facchino M, Popielak P, Panowski M, et al. The Environmental Impacts of Carbon Capture Utilization and Storage on the Electricity Sector: A Life Cycle Assessment Comparison between Italy and Poland. Energies 2022;15:6809. https://doi.org/10.3390/en15186809.

[17] Mac Dowell N, Fennell PS, Shah N, et al. The role of CO2 capture and utilization in mitigating climate change. Nat Clim Change 2017;7:243–9. https://doi.org/10.1038/nclimate3231.

[18] Wang Y, Pan Z, Zhang W, et al. Life cycle assessment of combustion-based electricity generation technologies integrated with carbon capture and storage: A review. Environ Res 2022;207:112219. https://doi.org/10.1016/j.envres.2021.112219.

[19] Becattini V, Gabrielli P, Mazzotti M. Role of Carbon Capture, Storage, and Utilization to Enable a Net-Zero-CO2-Emissions Aviation Sector. Ind Eng Chem Res 2021;60:6848–62. https://doi.org/10.1021/acs.iecr.0c05392.

[20] Gabrielli P, Gazzani M, Mazzotti M. The Role of Carbon Capture and Utilization, Carbon Capture and Storage, and Biomass to Enable a Net-Zero-CO2 Emissions Chemical Industry. Ind Eng Chem Res 2020;59:7033–45. https://doi.org/10.1021/acs.iecr.9b06579.

[21] Zhang X, Witte J, Schildhauer T, et al. Life cycle assessment of power-to-gas with biogas as the carbon source. Sustain Energy Fuels 2020;4:1427–36. https://doi.org/10.1039/C9SE00986H.

[22] Sitinjak C, Ebennezer S, Ober J. Exploring Public Attitudes and Acceptance of

CCUS Technologies in JABODETABEK: A Cross-Sectional Study. Energies 2023;16:4026. https://doi.org/10.3390/en16104026.

[23] Buchner GA, Stepputat KJ, Zimmermann AW, et al. Specifying Technology Readiness Levels for the Chemical Industry. Ind Eng Chem Res 2019;58:6957–69. https://doi.org/10.1021/acs.iecr.8b05693.

[24] Eikeland E, Blichfeld AB, Tyrsted C, et al. Optimized Carbonation of Magnesium Silicate Mineral for CO2 Storage. ACS Appl Mater Interfaces 2015;7:5258–64. https://doi.org/10.1021/am508432w.

[25] Stopic S, Dertmann C, Modolo G, et al. Synthesis of Magnesium Carbonate via Carbonation under High Pressure in an Autoclave. Metals 2018;8:993. https://doi.org/10.3390/met8120993.

[26] Olajire AA. A review of mineral carbonation technology in sequestration of CO2. J Pet Sci Eng 2013;109:364–92. https://doi.org/10.1016/j.petrol.2013.03.013.

[27] CO2 Sequestration by Mineral Carbonation: A Review. Glob NEST J 2018;20:497–503. https://doi.org/10.30955/gnj.002597.

[28] Reynes JF, Mercier G, Blais J-F, et al. Feasibility of a Mineral Carbonation Technique Using Iron-Silicate Mining Waste by Direct Flue Gas CO2 Capture and Cation Complexation Using 2,2′-Bipyridine. Minerals 2021;11:343. https://doi.org/10.3390/min11040343.

[29] Lackner KS, Butt DP, Wendt CH. Progress on binding CO2 in mineral substrates. Energy Convers Manag 1997;38:S259–64. https://doi.org/10.1016/S0196-8904(96)00279-8.

[30] Yadav S, Mehra A. Experimental study of dissolution of minerals and CO2 sequestration in steel slag. Waste Manag 2017;64:348–57. https://doi.org/10.1016/j.wasman.2017.03.032.

[31] Teir S, Eloneva S, Fogelholm C-J, et al. Fixation of carbon dioxide by producing hydromagnesite from serpentinite. Appl Energy 2009;86:214–8. https://doi.org/10.1016/j.apenergy.2008.03.013.

[32] Sanna A, Uibu M, Caramanna G, et al. A review of mineral carbonation technologies to sequester CO_2. Chem Soc Rev 2014;43:8049–80. https://doi.org/10.1039/C4CS00035H.

[33] Prigiobbe V, Polettini A, Baciocchi R. Gas–solid carbonation kinetics of Air Pollution Control residues for CO2 storage. Chem Eng J 2009;148:270–8. https://doi.org/10.1016/j.cej.2008.08.031.

[34] Ji L, Yu H, Yu B, et al. Insights into Carbonation Kinetics of Fly Ash from Victorian Lignite for CO2 Sequestration. Energy Fuels 2018;32:4569–78. https://doi.org/10.1021/acs.energyfuels.7b03137.

[35] Baras A, Li J, Ni W, et al. Evaluation of Potential Factors Affecting Steel Slag Carbonation. Processes 2023;11:2590. https://doi.org/10.3390/pr11092590.

[36] Rugabirwa B, Murindababisha D, Wang H, et al. A High-Pressure Gas–Solid Carbonation Route to Produce Vaterite. Cryst Growth Des 2019;19:242–8. https://doi.org/10.1021/acs.cgd.8b01314.

[37] Huijgen WJJ, Witkamp G-J, Comans RNJ. Mineral CO2 Sequestration by Steel Slag Carbonation. Environ Sci Technol 2005;39:9676–82. https://doi.org/10.1021/es050795f.

[38] Gerdemann SJ, O'Connor WK, Dahlin DC, et al. Ex Situ Aqueous Mineral Carbonation. Environ Sci Technol 2007;41:2587–93. https://doi.org/10.1021/es0619253.

[39] Pasquier L-C, Mercier G, Blais J-F, et al. Technical & economic evaluation of a mineral carbonation process using southern Québec mining wastes for CO2 sequestration of raw flue gas with by-product recovery. Int J Greenh Gas Control 2016;50:147–57. https://doi.org/10.1016/j.ijggc.2016.04.030.

[40] Zhao H, Park Y, Lee DH, et al. Tuning the dissolution kinetics of wollastonite via chelating agents for CO2 sequestration with integrated synthesis of precipitated calcium carbonates. Phys Chem Chem Phys 2013;15:15185–92. https://doi.org/10.1039/C3CP52459K.

[41] Pan S-Y, Chiang P-C, Chen Y-H, et al. Systematic Approach to Determination of Maximum Achievable Capture Capacity via Leaching and Carbonation Processes for Alkaline Steelmaking Wastes in a Rotating Packed Bed. Environ Sci Technol 2013;47:13677–85. https://doi.org/10.1021/es403323x.

[42] Ometto A, Batistella M, Filho AG, et al. Geotraceability and life cycle assessment in environmental life cycle management: towards sustainability. In: Loureiro G, Curran R, editors. Complex Syst. Concurr. Eng., London: Springer; 2007, p. 673–9. https://doi.org/10.1007/978-1-84628-976-7_74.

[43] Kleinekorte J, Fleitmann L, Bachmann M, et al. Life Cycle Assessment for the Design of Chemical Processes, Products, and Supply Chains. Annu Rev Chem Biomol Eng 2020;11:203–33. https://doi.org/10.1146/annurev-chembioeng-011520-075844.

[44] Kirchofer A, Brandt A, Krevor S, et al. Impact of alkalinity sources on the life-cycle energy efficiency of mineral carbonation technologies. Energy Environ Sci 2012;5:8631–41. https://doi.org/10.1039/C2EE22180B.

[45] Fernández-González J, Rumayor M, Domínguez-Ramos A, et al. The Relevance of Life Cycle Assessment Tools in the Development of Emerging Decarbonization Technologies. JACS Au 2023;3:2631–9. https://doi.org/10.1021/jacsau.3c00276.

[46] Hitch M, Dipple GM. Economic feasibility and sensitivity analysis of integrating industrial-scale mineral carbonation into mining operations. Miner Eng 2012;39:268–75. https://doi.org/10.1016/j.mineng.2012.07.007.

[47] Vega LF, Bahamon D, Alkhatib III. Perspectives on Advancing Sustainable CO2 Conversion Processes: Trinomial Technology, Environment, and Economy. ACS Sustain Chem Eng 2024;12:5357–82. https://doi.org/10.1021/acssuschemeng.3c07133.

[48] Zhou W, Pan L, Mao X. Optimization and Comparative Analysis of Different CCUS Systems in China: The Case of Shanxi Province. Sustainability 2023;15:13455. https://doi.org/10.3390/su151813455.

[49] Wang S, Wang M, Liu F, et al. A Review on the Carbonation of Steel Slag: Properties, Mechanism, and Application. Materials 2024;17:2066. https://doi.org/10.3390/ma17092066.

[50] Baciocchi R, Costa G, Di Bartolomeo E, et al. Wet versus slurry carbonation of EAF steel slag. Greenh Gases Sci Technol 2011;1:312–9. https://doi.org/10.1002/ghg.38.

[51] Pan S-Y, Chiang A, Chang E-E, et al. An Innovative Approach to Integrated Carbon Mineralization and Waste Utilization: A Review. Aerosol Air Qual Res 2015;15:1072–91. https://doi.org/10.4209/aaqr.2014.10.0240.

[52] Yin S, Aldahri T, Rohani S, et al. Insights into the Roasting Kinetics and Mechanism of Blast Furnace Slag with Ammonium Sulfate for CO2 Mineralization. Ind Eng Chem Res 2019;58:14026–36. https://doi.org/10.1021/acs.iecr.9b03109.

[53] Molahid VLM, Kusin FM, Soomro MH. Mineral carbonation for carbon dioxide capture and storage using mining waste as feedstock material. IOP Conf Ser Earth Environ Sci 2023;1205:012011. https://doi.org/10.1088/1755-1315/1205/1/012011.

[54] Tiefenthaler J, Braune L, Bauer C, et al. Technological Demonstration and Life Cycle Assessment of a Negative Emission Value Chain in the Swiss Concrete Sector. Front Clim 2021;3. https://doi.org/10.3389/fclim.2021.729259.

[55] Zhan B, Poon CS, Liu Q, et al. Experimental study on CO2 curing for enhancement of recycled aggregate properties. Constr Build Mater 2014;67:3–7. https://doi.org/10.1016/j.conbuildmat.2013.09.008.

[56] Ben Ghacham A, Pasquier L-C, Cecchi E, et al. Valorization of waste concrete through CO2 mineral carbonation: Optimizing parameters and improving reactivity using concrete separation. J Clean Prod 2017;166:869–78. https://doi.org/10.1016/j.jclepro.2017.08.015.

[57] Yu C, Cai L, Jiang G, et al. Mineral carbonation of CO2 with utilization of coal gasification slags based on chemical looping. Asia-Pac J Chem Eng 2021;16:e2636. https://doi.org/10.1002/apj.2636.

[58] Ostovari H, Sternberg A, Bardow A. Rock 'n' use of CO_2 : carbon footprint of carbon capture and utilization by mineralization. Sustain Energy Fuels 2020;4:4482–96. https://doi.org/10.1039/D0SE00190B.

[59] Fagerlund J, Nduagu E, Romão I, et al. CO2 fixation using magnesium silicate minerals part 1: Process description and performance. Energy 2012;41:184–91. https://doi.org/10.1016/j.energy.2011.08.032.

[60] Wang X, Maroto-Valer MM. Dissolution of serpentine using recyclable ammonium salts for CO2 mineral carbonation. Fuel 2011;90:1229–37. https://doi.org/10.1016/j.fuel.2010.10.040.

[61] Wang R, Jin P, Dong H, et al. Effect of moist content on the bio-carbonated steel slag bricks. Constr Build Mater 2021;269:121313. https://doi.org/10.1016/j.conbuildmat.2020.121313.

[62] Angelidaki I, Treu L, Tsapekos P, et al. Biogas upgrading and utilization: Current status and perspectives. Biotechnol Adv 2018;36:452–66. https://doi.org/10.1016/j.biotechadv.2018.01.011.

[63] Informatics NO of D and. NIST Chemistry WebBook n.d. https://webbook.nist.gov/chemistry/ (accessed April 28, 2025).

[64] Lugo-Méndez H, Lopez-Arenas T, Torres-Aldaco A, et al. Interstage Pressures of a Multistage Compressor with Intercooling. Entropy 2021;23:351. https://doi.org/10.3390/e23030351.

[65] Individual & Universal Gas Constants: Definitions, Values, and Applications n.d. https://www.engineeringtoolbox.com/individual-universal-gas-constant-d_588.html (accessed April 28, 2025).

[66] Boyce MP. Gas turbine engineering handbook. 4th ed. Amsterdam, Boston: Elsevier/Butterworth-Heinemann; 2012.

[67] Yahya NA, Daas OM, Alboum NOF, et al. Design of Vertical Pressure Vessel Using ASME Codes. AIJR Proc 2018.

[68] Davis JR. Surface Engineering of Specialty Steels. In: Cotell CM, Sprague JA, Smidt FA, editors. Surf. Eng., ASM International; 1994, p. 762–75. https://doi.org/10.31399/asm.hb.v05.a0001306.

[69] Legendre D, Zevenhoven R. Assessing the energy efficiency of a jaw crusher. Energy 2014;74:119–30. https://doi.org/10.1016/j.energy.2014.04.036.

[70] Mining & Mineral Processing Equipment Manufacturer - JXSC Mine Machinery. JXSC Mach n.d. https://www.jxscmachine.com/ (accessed May 1, 2025).

[71] Emissions trading n.d. https://www.emissionshandelsregister.at/en/emissionstrading (accessed April 30, 2025).

[72] Yildirim IZ, Prezzi M. Chemical, Mineralogical, and Morphological Properties of Steel Slag. Adv Civ Eng 2011;2011:463638. https://doi.org/10.1155/2011/463638.

[73] Drizo A, Cummings J, Weber D, et al. New Evidence for Rejuvenation of Phosphorus Retention Capacity in EAF Steel Slag. Environ Sci Technol 2008;42:6191–7. https://doi.org/10.1021/es800232r.

[74] Steelmaking slag as a permanent sequestration sink for carbon dioxide - ProQuest n.d. https://www.proquest.com/openview/ae473362e9079bfc554f7186f493347e/1?pq-origsite=gscholar&cbl=1056347 (accessed April 30, 2025).

[75] Home. PROSPIN n.d. https://www.rpb-prospin.com/ (accessed May 1, 2025).

[76] ISO 14040:2006. ISO n.d. https://www.iso.org/standard/37456.html (accessed May 19, 2025).

[77] Shonhiwa C, Mapantsela Y, Makaka G, et al. Biogas Valorisation to Biomethane for Commercialisation in South Africa: A Review. Energies 2023;16:5272. https://doi.org/10.3390/en16145272.

[78] Pauliuk S, Kondo Y, Nakamura S, et al. Regional distribution and losses of end-of-life steel throughout multiple product life cycles—Insights from the global multiregional MaTrace model. Resour Conserv Recycl 2017;116:84–93. https://doi.org/10.1016/j.resconrec.2016.09.029.

[79] LCA-ActivityBrowser/activity-browser 2025.

[80] MATLAB n.d. https://de.mathworks.com/products/matlab.html (accessed May 19,

2025).

[81] Kettner C, Böheim M, Sommer M, et al. Transformation to a renewable electricity system in Austria: Insights from an integrated model analysis. Renew Energy 2024;223:119957. https://doi.org/10.1016/j.renene.2024.119957.

[82] Gaspreisindizes: AEA - Österreichische Energieagentur n.d. https://www.energyagency.at/fakten/gaspreisindizes (accessed May 3, 2025).

[83] EU Carbon Permits - Price - Chart - Historical Data - News n.d. https://tradingeconomics.com/commodity/carbon (accessed May 3, 2025).

[84] Steuern & Finanzen n.d. https://www.usp.gv.at/themen/steuern-finanzen.html (accessed May 3, 2025).

[85] Austria Interest Rate n.d. https://tradingeconomics.com/austria/interest-rate (accessed May 3, 2025).

[86] Deng H, Roussanaly S, Skaugen G. Techno-economic analyses of CO2 liquefaction: Impact of product pressure and impurities. Int J Refrig 2019;103:301–15. https://doi.org/10.1016/j.ijrefrig.2019.04.011.

[87] Cost Analysis of Driverless Truck Operations n.d. https://doi.org/10.1177/0361198120930228.

[88] CO2 and Dry Ice Solutions n.d. https://www.ascoco2.com/en/ (accessed April 30, 2025).

[89] Dai H, Li N, Wang Y, et al. The Analysis of Three Main Investment Criteria: NPV IRR and Payback Period, Atlantis Press; 2022, p. 185–9. https://doi.org/10.2991/aebmr.k.220307.028.

[90] Sihombing FDW Yusri Bin Arshad, Haeryip. Monte Carlo Net Present Value for Techno-Economic Analysis of Oil and Gas Production Sharing Contract. IJTech - Int J Technol n.d. https://ijtech.eng.ui.ac.id/article/view/2051 (accessed May 3, 2025).

[91] Nasirly R, Prendika W. Feasibility Study of Agropolymer Bricks from Silica Palm Ash for Sustainable Material (case Studi in Pelalawan), 2023.

[92] Marketing. Recycled Concrete Aggregates - Recycling Concrete. Fibo Intercon 2019. https://fibointercon.com/articles/recycled-concrete-aggregate/ (accessed May 21, 2025).

[93] Mike. Calcium carbonate price index. Businessanalytiq 2021. https://businessanalytiq.com/procurementanalytics/index/calcium-carbonate-price-index/ (accessed May 3, 2025).

Appendix

Table A.1: Summary of LCI data and impact categories

Product	Name of data set	Location	Data base	Carbon footprint	Considered impact
Electricity	Electricity, medium voltage	AT	Ecoinvent via Activity browser (v. 2.9.0)	243 gr CO2 eq. /kWh	Global warming potential (GWP100)
Electricity	Electricity production, hydro, run-of-river	AT	Ecoinvent via Activity browser (v. 2.9.0)	4.2 gr CO2 eq. /kWh	Global warming potential (GWP100)
Electricity	Electricity production, hydro, reservoir, alpine region	AT	Ecoinvent via Activity browser (v. 2.9.0)	6.3 gr CO2 eq. /kWh	Global warming potential (GWP100)
Electricity	electricity production, wind, >3MW turbine, onshore	AT	Ecoinvent via Activity browser (v. 2.9.0)	29 gr CO2 eq. /kWh	Global warming potential (GWP100)
Electricity	heat and power co-generation, wood chips,	AT	Ecoinvent via Activity browser (v. 2.9.0)	54 gr CO2 eq. /kWh	Global warming potential (GWP100)
Electricity	electricity production, deep geothermal	AT	Ecoinvent via Activity browser (v. 2.9.0)	69.9 gr CO2 eq. /kWh	Global warming potential (GWP100)
Electricity	electricity, high voltage, production mix	AT	Ecoinvent via Activity browser (v. 2.9.0)	139.9 gr CO2 eq. /kWh	Global warming potential (GWP100)
Electricity	heat and power co-generation, biogas, gas engine	AT	Ecoinvent via Activity browser (v. 2.9.0)	227.8 gr CO2 eq. /kWh	Global warming potential (GWP100)
Electricity	heat and power co-generation, natural gas	AT	Ecoinvent via Activity browser (v. 2.9.0)	541.6 gr CO2 eq. /kWh	Global warming potential (GWP100)
Electricity	heat and power co-generation, oil	AT	Ecoinvent via Activity browser (v. 2.9.0)	1018 gr CO2 eq. /kWh	Global warming potential (GWP100)
Electricity	heat and power co-generation, hard coal	AT	Ecoinvent via Activity browser (v. 2.9.0)	1153 gr CO2 eq. /kWh	Global warming potential (GWP100)

Cooling Energy	Cooling energy, from natural gas, at co-gen unit with absorption chiller 100kW	RER	Ecoinvent via Activity browser (v. 2.9.0)	68.6 gr CO2 eq. /MJ	Global warming potential (GWP100)
Heat, district or industrial, natural gas	Heat and power co-generation, natura gas, combined cycle, power plant	AT	Ecoinvent via Activity browser (v. 2.9.0)	27.7 gr CO2 eq. /MJ	Global warming potential (GWP100)
Transport	Transport, freight, lorry 16-32 metric ton EUR 6	RER	Ecoinvent via Activity browser (v. 2.9.0)	100.2 gr CO2 eq. /(km.ton)	Global warming potential (GWP100)
Steel	Steel production, electric, low alloyed	AT	Ecoinvent via Activity browser (v. 2.9.0)	315.28 gr CO2 eq. /kg	Global warming potential (GWP100)
Steel	Steel, chromium steel 18/8	RER	Ecoinvent via Activity browser (v. 2.9.0)	4282.1 gr CO2 eq. /kg	Global warming potential (GWP100)
Metal Working	Metal working, average for steel product manufacturing	RER	Ecoinvent via Activity browser (v. 2.9.0)	1508.8 gr CO2 eq. /kg	Global warming potential (GWP100)
Metal Working	Metal working, average for chromium steel manufacturing	RER	Ecoinvent via Activity browser (v. 2.9.0)	2138.4 gr CO2 eq. /kg	Global warming potential (GWP100)

Table A.2: LCI by Size Fraction and Steel Recovery

RCA size Fraction (mm)	Technosphere flows	Unit	Location	Without steel recovery at the end of plant life		With 95% steel recovery at the end of plant life	
				Carbonation	Crusher	Carbonation	Crusher
0.0 - 0.065	electricity, medium voltage	kWh	AT	0.0075	0.323611	0.0075	0.323611
	Steel, low-alloyed	kg	AT	0.000112	0.000425	0.000006	0.000021
	metal working, avarage for metal product manufacturing	kg	RER	0.000112	0.000425	0.000006	0.000021
0.065-0.125	electricity, medium voltage	kWh	AT	0.011278	0.335000	0.011278	0.335000
	Steel, low-alloyed	kg	AT	0.000142	0.000542	0.000007	0.000027
	metal working, avarage for metal product manufacturing	kg	RER	0.000142	0.000542	0.000007	0.000027
0.125 - 0.250	electricity, medium voltage	kWh	AT	0.012889	0.257222	0.012889	0.257222
	Steel, low-alloyed	kg	AT	0.000154	0.000589	0.000008	0.000029
	metal working, avarage for metal product manufacturing	kg	RER	0.000154	0.000589	0.000008	0.000029
0.250 - 0.5	electricity, medium voltage	kWh	AT	0.017194	0.223889	0.017194	0.223890
	Steel, low-alloyed	kg	AT	0.000183	0.000698	0.000009	0.000035
	metal working, avarage for metal product manufacturing	kg	RER	0.000183	0.000698	0.000009	0.000035
0.5 - 1.0	electricity, medium voltage	kWh	AT	0.024083	0.193333	0.024083	0.193333
	Steel, low-alloyed	kg	AT	0.000224	0.000854	0.000011	0.000043

	metal working, avarage for metal product manufacturing	kg	RER	0.000224	0.000854	0.000011	0.000043
1.0 - 2.0	electricity, medium voltage	kWh	AT	0.030083	0.141667	0.030083	0.141667
	Steel, low-alloyed	kg	AT	0.000256	0.000977	0.000013	0.000049
	metal working, avarage for metal product manufacturing	kg	RER	0.000256	0.000977	0.000013	0.000049
2.0 - 4.0	electricity, medium voltage	kWh	AT	0.032833	0.070833	0.032833	0.070833
	Steel, low-alloyed	kg	AT	0.000270	0.001030	0.000014	0.000051
	metal working, avarage for metal product manufacturing	kg	RER	0.000270	0.001030	0.000014	0.000051

Table A.3: LCI by Pressure under 95% Steel Recovery

Unit Operation	Technosphere flows	Unit	Location	CO_2 delivery pressure (bar)									
				7	10	15	20	25	30	40	50	60	70
Liquefaction	Electricity, medium voltage	kWh	AT	0.0519	0.0579	0.0630	0.0672	0.0705	0.0727	0.0759	0.0782	0.0801	0.0824
	Cooling energy	mega-joule	RoW	0.6775	0.6929	0.6767	0.6721	0.6674	0.6576	0.6380	0.6150	0.5936	0.5957
	Steel, chromium steel	kg	RER	5.33E-07	6E-07	6.6E-07	7E-07	7.2E-07	7.6E-07	8.1E-07	8.3E-07	8.4E-07	8.5E-07
	Metal working, average for chromium steel product	kg	RER	5.33E-07	6E-07	6.6E-07	7E-07	7.2E-07	7.6E-07	8.1E-07	8.3E-07	8.4E-07	8.5E-07
Evaporation	Heat, district or industrial, natural gas	mega-joule	AT	0.42917	0.4094	0.3844	0.3646	0.3479	0.3323	0.3042	0.2792	0.2531	0.2208
	Steel, chromium steel 18/8	kg	RER	3.367E-07	3.3E-07	3.2E-07	3.1E-07	3E-07	2.9E-07	2.7E-07	2.6E-07	2.5E-07	2.3E-07
	Metal working, average for chromium steel product	kg	RER	3.367E-07	3.3E-07	3.2E-07	3.1E-07	3E-07	2.9E-07	2.7E-07	2.6E-07	2.5E-07	2.3E-07